BSD-TR-67-182

8525-2-T

PHYSICAL OPTICS APPLIED TO CONE-SPHERE-LIKE OBJECTS

Technical Report No. 2

F 04694-67-C-0055

Captain J. Wheatley, Contract Monitor

By

T.B.A. Senior

May 1967

Prepared for

Department of the Air Force
Space and Missile Systems Organization (AFSC)
Norton Air Force Base, California 92409

ABSTRACT

The physical optics method is applied to a variety of cone-sphere-like objects, and the resulting expressions for the back scattered field are examined.

FOREWORD

This report (BSD-TR-67-182) was prepared by the Radiation Laboratory of the Department of Electrical Engineering, The University of Michigan. The work was performed under Contract F 04694-67-C-0055, "Investigation of Re-entry Vehicle Surface Fields (Backscatter) (SURF) ". Dr. Raymond F. Goodrich is the Principal Investigator and Mr. Burton A. Harrison, Contract Manager. The work was administered under the direction of the Air Force Space and Missile Systems Organization (AFSC), Norton Air Force Base, California, 92409 by Captain James Wheatley and was monitored by H. J. Katzman of the Aerospace Corporation.

This document is subject to special export controls and each transmittal to foreign governments or foreign nationals may be made only with prior approval of Space and Missile Systems Organization (SMSDI), Los Angeles Air Force Station, Los Angeles, California 90045.

Information in this report is embargoed under the Department of State International Traffic in Arms Regulations. Private individuals or firms require a Department of State export license.

The publication of this report does not constitute Air Force Approval of the report's findings or conclusions. It is published for the exchange and stimulation of ideas.

SAMSO Approving Authority.

William J. Schlerf

WILLIAM J. SCHLERF
CONTRACTING OFFICER

TABLE OF CONTENTS

I
INTRODUCTION

One of the most common and useful techniques for estimating the scattering behavior of an object at frequencies for which all of the "effective" dimensions are large compared with the wavelength is the physical optics method. This is basically an extension of geometrical optics in which an explicit form for the surface field over the entire object is assumed, thereby reducing the determination of the scattered field to quadratures. In view of the sweeping nature of this assumption, it is not surprising that the results are only approximate and, in many cases, grossly in error. Nevertheless, the method is universal and direct, and perhaps the truly surprising thing is the accuracy that is sometimes obtained by thoughtful and selective application of the technique, often under circumstances when it would appear that the conditions postulated in arriving at the assumed form for the surface field distribution are violated.

Geometrical optics is, as its name implies, a ray technique. If there is a smooth convex (or concave) surface normal to the incident field direction, this will give rise to a specular return, and from a consideration of the power reduction in the ray bundle produced by the divergence of the scattered beam, the cross section is found to be

$$\sigma = \pi R_1 R_2 \tag{1}$$

where R_1 and R_2 are the principal radii of curvature of the surface. The polarization of the scattered field is the same as if the reflection had taken place at an infinite tangent plane. For a restricted class of bodies it can be verified that (1) is the correct leading term in the asymptotic expansion of the cross section for small wavelengths.

According to geometrical optics, the back scattering cross section is zero at aspects other than those for which a specular reflection occurs, and a natural extension of the method which serves to provide continuity of aspect coverage in the cross section prediction is to assume that the fields indicated by geometrical optics are excited at all points of the surface. This is the physical optics approximation. It is equivalent to assuming that each element of surface scatters as though part of the infinite tangent plane at that point, and leads to a surface current having the value

$$\underline{J} = 2(\hat{n} \times \underline{H}^i) \tag{2}$$

at each point of the illuminated region, where $\hat{n}$ is the unit vector normal to the surface and $\underline{H}^i$ is the incident magnetic vector. This current is taken as zero within the shadow. Since the surface field is now specified in its entirety, the calculation of the scattered field is reduced to quadratures.

If the application of physical optics were limited to those cases where the postulated surface fields are uniformly valid, the usefulness of this method would be small indeed. All bodies with surface singularities would obviously be ruled out, and for smooth convex shapes the assumption of an abrupt discontinuity at the shadow boundary, in place of the continuous but rapid transition that actually occurs in this region, would force us to omit all situations where shadowing is present. We are then left with only such infinite bodies as the paraboloid, and even here the permissible range of aspects is restricted.

In practice, however, physical optics is a great deal more valuable than would appear from these remarks, and is the basis for most techniques for cross section estimation. We shall now apply it to the determination of the back scattering cross section of the cone-sphere-like objects of interest under the present program, taking first the case of nose-on incidence, and separating out the contributions associated with the tip, the join and the shadow boundary. By virtue of the postulated current, each element of the surface contributes to the scattering independently of its neighbors (except insofar as such neighbors may shadow the chosen element), and this justifies us in breaking up the target into component parts should it prove convenient to do so.

II
NOSE-ON INCIDENCE

For a body of revolution illuminated by a plane wave traveling in the direction of the axis of symmetry (nose-on incidence), the general expression for the back scattered field (Crispin et al, 1959) simplifies considerably, and if the surface is defined by the equation

$$\rho = \rho(z) \tag{3}$$

with $\rho = \sqrt{x^2 + y^2}$ (see Fig. 1), the back scattered electric vector in

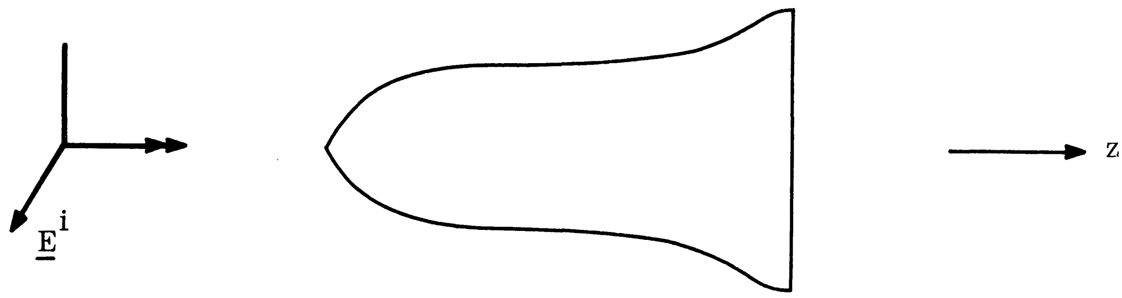

FIG. 1

the far field can be written as

$$\underline{E}^s = \hat{x} E^s , \qquad E^s = \frac{e^{ikR}}{kR} \left\{ ik^2 \int_{z_1}^{z_2} e^{2ikz} \left(\rho \frac{\partial \rho}{\partial z} \right) dz \right\} \tag{4}$$

where the integration is in the direction of the incident propagation vector (so that $z_2 > z_1$) and is carried out over the illuminated portion of the body. The bracketed quantity in (4) is simply the far field amplitude, and if this is denoted by S, then

$$S = \frac{4i\pi^2}{\lambda^2} \int_{z_1}^{z_2} e^{2ikz} \left(\rho \frac{\partial \rho}{\partial z} \right) dz , \tag{5}$$

which can be written alternatively as

$$S = \frac{2i\pi}{\lambda^2} \int_{z_1}^{z_2} e^{2ikz} \frac{\partial A}{\partial z} dz \tag{6}$$

where $A = \pi\rho^2$ is the sectional area of the body. In terms of S, the radar back scattering cross section is

$$\sigma = \frac{\lambda^2}{\pi} |S|^2 \quad . \tag{7}$$

When the physical optics integral is evaluated, it is found that three different types of surface region can produce contributions. They are (i) places where $A(z)$ is stationary with respect to z; (ii) places where A, or any of its derivatives, is discontinuous, and (iii) the end points of the range of integration. The first of these regions leads to a specular contribution, and one of the greatest usefulnesses of the physical optics method is for the calculation of such returns and the sidelobes thereof. The second type of region is an important feature of any pointed shape and, as we shall see, the associated high frequency return decreases with the increasing order of the first discontinuous derivative of the profile $\rho(z)$. Note that $\rho(z)$, and hence $A(z)$, must be continuous if the surface is to be conjoint, though any (or all) derivatives may be discontinuous. It is not uncommon for one of these places to coincide with an end point of the range of integration, from which the third category of contribution arises, but even if A is physically continuous there, along with its derivatives, the end still contributes by virtue of the abrupt change implied by the cessation of integration, or, in the case of a shadow boundary, because of the discontinuity introduced by the physical optics approximation to the surface field.

Given an analytical expression for the physical optics integral, it is possible to identify the portions of the surface responsible for the scattering by examining the phase factors of the individual terms. These terms can then be associated with the specific local surface features giving rise to them, and when such features lie in regions where the postulated surface field is known to be in error, the terms can be ignored or, preferably, replaced by others based on more realistic values for the fields.

To illustrate this procedure, consider a sphere of radius a. If the origin of coordinates and, hence, of phase, is taken to be at the center of the sphere, the physical optics expression for the far field amplitude in the back scattering direction can be obtained from (5) by putting

$$\rho = \sqrt{a^2 - z^2}, \qquad z_1 = -a, \qquad z_2 = 0 \ .$$

We then have

$$S = -\frac{4i\pi^2}{\lambda^2} \int_{-a}^{0} e^{2ikz} z\, dz$$

which can be evaluated to give

$$S = -\frac{ka}{2}\left(1 - \frac{i}{2ka}\right) e^{-2ika} - \frac{i}{4} \quad . \tag{8}$$

The first group of terms has a phase factor corresponding to a reflection from the front face of the sphere and is, in fact, the specular return. To the order shown it is identical to the result derived (Senior, 1965) from the exact Mie series solution. The last term in (8) has the same magnitude as the correction to the specular contribution, but its phase is that appropriate to scattering from the shadow boundary. Since the optics approximation is in error in this region, the term is suspect, and a more refined analysis leads to a shadow boundary contribution which is quite distinct from this, and is exponentially attenuated for large ka. We can therefore omit the last term of (8) at high frequencies, and the back scattering cross section is then given by the first group of terms alone. At somewhat lower frequencies, however, a valid estimate of the shadow boundary effect must be introduced.

Let us now consider the case of a flat-backed cone (see Fig. 2). If the height and half-angle are h and α respectively, then

$$\rho = z\tan\alpha\,, \qquad z_1 = 0\,, \qquad z_2 = h$$

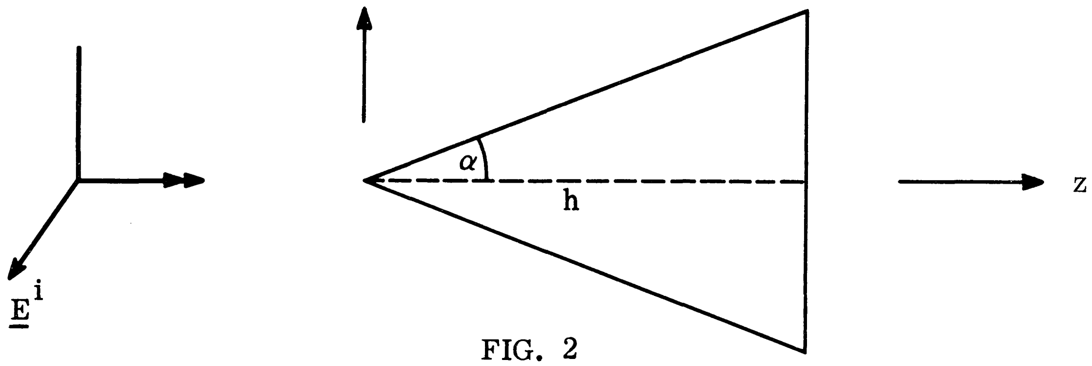

FIG. 2

where the phase origin has been taken to be at the vertex. The corresponding expression for S is

$$S = \frac{4i\pi^2}{\lambda^2}\tan^2\alpha\int_0^h e^{2ikz}\,z\,dz$$

$$= -\frac{i}{4}\tan^2\alpha\left\{1 + e^{2ikh}(2ikh - 1)\right\} \tag{9}$$

and from an inspection of the phase factors of the individual terms it is seen that (9) implies a far field amplitude

$$-\frac{i}{4}\tan^2\alpha \tag{10}$$

associated with the tip, and a far field amplitude

$$-\frac{i}{4}\tan^2\alpha(2ikh - 1)e^{2ikh} \tag{11}$$

appropriate to the rim singularity at the base. For large kh the latter is approximately

$$\frac{\pi h}{\lambda} \tan^2\alpha \, e^{2ikh} \tag{12}$$

which dominates the overall return at high frequencies due to its wavelength dependence. The rim is, however, both a surface singularity and the shadow boundary, and on either score the estimated scattering is suspect. As we have seen, a shadow boundary per se is only a negligible contributor at high frequencies, but the failure of the physical optics approximation to reproduce the essential features of the surface field in the vicinity of an edge is a more serious shortcoming which invalidates the estimate of the rim return even for some other types of capped cone for which the rim and shadow boundary do not coincide. Here again it is necessary to refine the physical optics estimate of the scattering.

The tip contribution is, however, another matter. In the limit of a semi-infinite cone ($h = \infty$) no return can come from the termination, and the second part of (9) must be ignored. This is usually justified on a mathematical basis by attributing a non-zero conductivity to the surrounding medium (giving k a positive imaginary part), so that the appropriate terms in (9) are exponentially attenuated through through the factor e^{2ikh}. The only return is now provided by the tip, and from (10) we have

$$\sigma_{tip} = \frac{\lambda^2}{16\pi} \tan^4\alpha \tag{13}$$

which is the well-known tip answer.

As with any physical optics result, we can attempt to judge the accuracy of the predicted scattering from the tip by comparing the actual currents in its vicinity with the postulated distribution. Unfortunately, the findings in this case are somewhat ambiguous. Probe measurements show that close to the tip the currents depart significantly from the optics values, and it may be necessary to go two (or more) wavelengths along the generators before these limiting values are achieved. On this evidence, therefore, equation (13) is suspect, but since the expression (10) for the far field amplitude is in precise agreement with the results deduced from the exact solution for a semi-infinite cone (Felsen, 1955) for both large and small cone angles (see Kleinman and Senior, 1963), it must be concluded that (10), and hence (13), is in fact correct. Note, however, that the resulting tip scatter is too small to be of interest for most practical purposes, For example, when $\alpha = 11^{o}$, σ_{tip} is $3.16 \times 10^{-8} m^2$ at 10 Gc, rising only to $3.16 \times 10^{-4} m^2$ at 100 Mc, and by comparison the return from almost any feasible type of cone termination is dominant.

With terminations other than a flat back, the physical optics estimate (9) is unaffected unless a portion of the cap is in the illuminated region, and consequently for a spherically-capped cone with the origin of the sphere at the apex of the cone (or, indeed, on the axis of the cone at any distance X from the apex with $0 \leq X \leq h$), the predicted far field amplitude is identical to that in (9). But if the sphere is chosen to have its origin at a distance $X > h$ from the apex, with radius

$$\left\{ (h \tan\alpha)^2 + (X-h)^2 \right\}^{1/2} ,$$

so as to achieve a join to the cone with a discontinuity in at most the first derivative of the profile, a part of the sphere is visible, and the physical optics return is changed accordingly. From equation (5) with

$$\rho = \left\{ (h \tan\alpha)^2 + (X-h)^2 - (X-z)^2 \right\}^{1/2} , \quad z_1 = h, \quad z_2 = X$$

(see Fig. 3) we have, for the cap alone

$$S = \frac{i}{4} \left\{ e^{2ikh} \left(2ik(X-h) + 1 \right) - e^{2ikX} \right\} \tag{14}$$

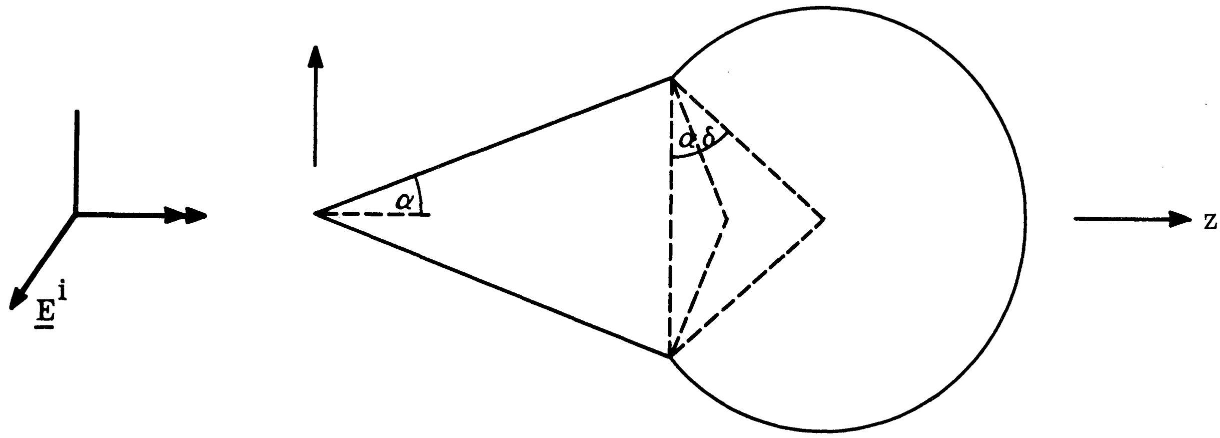

FIG. 3

valid for $X > h$, and when added to the cone contribution (9), the far field amplitude for the spherically-capped body is found to be

$$S = -\frac{i}{4}\left\{\tan^2\alpha - e^{2ikh}\left(2ik(X - h\sec^2\alpha) + \sec^2\alpha\right) + e^{2ikX}\right\}. \tag{15}$$

The first term in (15) is again the tip contribution and is believed accurate. The third term originates at the shadow boundary; apart from the phase factor associated with the choice of origin at the vertex of the cone, it is identical to the result previously found for a sphere in isolation, and is erroneous for the reason already given. The middle group of terms is more interesting, however. Its phase factor identifies it as a contribution from the join of the cone and sphere, and its magnitude depends on the nature of this join through the parameter X. In general, as seen from (15),

$$S_{join} = \frac{i}{4}\left\{2ik(X - h\sec^2\alpha) + \sec^2\alpha\right\} e^{2ikh}, \tag{16}$$

but in the special case when the cone and sphere are smoothly mated to produce continuity of the first derivative of the profile across the join, $X = h\sec^2\alpha$ and equation (16) reduces to

$$S_{join} = \frac{i}{4} \sec^2\alpha \, e^{2ikh} \quad . \tag{17}$$

The body is now a cone-sphere—a shape which has achieved such a classical status in nose-cone studies that the term is often used in a generic sense to embrace an entire class of smoothly terminated cones. In the present work, however, the description cone-sphere will be limited to the specific body detailed above.

Although the first derivative of the profile is continuous at the join, the second and all higher derivatives are discontinuous there, and in particular the radius of curvature is also discontinuous. Even for a cone-sphere, therefore, the join is still a physical singularity (albeit a concealed one), and it would not be unreasonable to expect that the contribution (17) is in error just as it is for a flat-backed cone. On the other hand, the join is now entirely in the illuminated region, which gives some confidence in the accuracy of the current distribution assumed locally, and detailed analyses of back scattering data for 30^o and 25^o cone-spheres as functions of frequency (Gent et al, 1960; Senior, 1963) have shown the cross sections to be consistent with a join contribution of the form given here. The latter check is admittedly somewhat qualitative, but recent probe measurements near to the join have confirmed the overall accuracy of the physical optics approximation beyond any doubt, and even for values of ka as small as 3 the perturbation produced by the singularity is relatively insignificant. In essence, it would appear that the perturbation to the optics distribution which, for a wedge singularity, is of order unity, is reduced to a level $O(1/ka)$ or less when the discontinuity is in the second derivative of the profile. It is therefore concluded that equation (17) provides a valid high frequency estimate of the scattering from this part of the surface, though it should be noted that this would no longer be true if any portion of the surface beyond the join were to reflect a substantial amount of energy back toward it.

At frequencies sufficiently high for the shadow boundary (creeping wave) return to be neglected, we now have, for the far field amplitude of a cone-sphere,

$$S = -\frac{i}{4}\left(\tan^2\alpha - \sec^2\alpha\, e^{2ikh}\right), \tag{18}$$

and whereas the tip and join contributions have the same wavelength dependence, the latter is considerably larger in magnitude for all cone-spheres of practical interest. Indeed,

$$\sigma_{join} = \frac{\lambda^2}{16\pi}\sec^4\alpha \tag{19}$$

(cf equation 13), and when $\alpha = 11^o$, σ_{join} exceeds σ_{tip} by a factor of about 750. We can therefore disregard σ_{tip} by comparison and use (19) as a high frequency estimate of the cross section of the entire cone-sphere. For small cone angles

$$\sigma \sim 0.02\lambda^2 , \tag{20}$$

which is approximately one-half that which would have been obtained if the spurious shadow boundary term in (15) had not been ignored. Failure to omit this term may be the reason for the larger high frequency estimate suggested by Siegel (1963).

Let us now return to a consideration of the join contribution (16) for a general spherically-capped cone. If $X > h\sec^2\alpha$ the cap is more bulbous than for a cone-sphere, and the shape is as depicted in Fig. 3; conversely, if $X < h\sec^2\alpha$ the cap is less bulbous. In either case it is convenient to express X in terms of the angle δ between the tangents to the cone and sphere at the join to give

$$X - h\sec^2\alpha = \frac{h\sec^2\alpha\tan\alpha\tan\delta}{1-\tan\alpha\tan\delta}$$

$$\simeq h\sec^2\alpha\tan\alpha\tan\delta \tag{21}$$

providing $\tan\alpha\tan\delta \ll 1$. δ is positive or negative according as the cap is more or less bulbous respectively than for a cone-sphere, and on inserting (21) into (16) we have

$$S_{join} \simeq \frac{i}{4} \sec^2\alpha(1+2ikh\tan\alpha\tan\delta)\, e^{2ikh} . \tag{22}$$

A ridge or kink equivalent to an angular difference δ will therefore increase the join contribution from a cone-sphere, and hence the high frequency estimate of the overall scattering, by a factor

$$1+2ikh\tan\alpha\tan\delta ,$$

and at sufficiently high frequencies the second term will dominate by virtue of its kh factor, so that ultimately

$$S_{join} \simeq -\frac{\pi h}{\lambda} \sec^2\alpha\tan\alpha\tan\delta\, e^{2ikh} \tag{23}$$

There is, however, danger in a straightforward acceptance of this result. The join contribution now has the same wavelength dependence as the return from the rim of a flat-backed cone (see equation 12). It is also similar in magnitude if δ is comparable to α but, as we have already noted, the physical optics estimate of rim scattering is erroneous primarily because of the failure of the assumed current distribution to take account of the significant surface field reflection at a wedge-type singularity. This reflection certainly decreases with decreasing δ, and though there is some question whether the physical optics prediction is ever valid if $\delta \neq 0$, it is pertinent to remark that (23) is almost identical to the result obtained by Dawson et al (1960) using the more accurate circular wedge approximation. It would therefore appear that (22) does give a valid estimate of the join contribution providing δ is small, and this now shows the importance of accurate construction in the region of the join if the expected cone-sphere behavior is to be achieved. This region is, without doubt, the most critical one for a cone-sphere, and some of the irregularities in the experimental data of Gent et al (1960) may have been due to imperfections amongst the 50 models employed in their study.

The cone-sphere is, of course, only one particular form of terminated cone, and though it is usually taken as the prototype of a nose-cone, this is more for the simplicity of its design than for its optimum characteristics. It is certainly not true that its nose-on cross section is the lowest attainable with a metallic body of the same gross dimensions, and since the magnitude of the scattering from the join is a major factor in determining the overall cross section, it is of interest to examine the effect of cone terminations other than a smoothly-mated sphere. For this purpose a general treatment is desirable.

Let us assume that in the vicinity of the join at least the cap is defined by the equation

$$\rho^2 = \sum_{n=0}^{\infty} a_n (z-h)^n \tag{24}$$

where the a_n are constant and, to make the surface continuous with that of the cone

$$a_o = (h \tan\alpha)^2 \; . \tag{25}$$

If equation (24) holds over a region extending up to and beyond the shadow boundary, the only physical optics contributions provided by the cap are those associated with the join and shadow boundary, and for the former we have

$$S_{join} = \frac{4i\pi^2}{\lambda^2} \int_h e^{2ikz} \left(\rho \frac{\partial\rho}{\partial z}\right) dz \; .$$

Inserting the expression (24) for ρ^2,

$$S_{join} = \frac{2i\pi^2}{\lambda^2} \sum_{n=1}^{\infty} n\, a_n \int_h e^{2ikz} (z-h)^{n-1}\, dz \; ,$$

and since

$$\int_h e^{2ikz}(z-h)^{n-1}\,dz = \frac{n-1}{-2ik}\int_h e^{2ikz}(z-h)^{n-2}\,dz$$

$$= \frac{(n-1)!}{(-2ik)^n}\, e^{2ikh} \quad ,$$

it follows that

$$S_{join} = \frac{2i\pi^2}{\lambda^2}\sum_{n=1}^{\infty} a_n \frac{(n-1)!}{(-2ik)^n}\, e^{2ikh} \quad . \tag{26}$$

If we now add the join contribution (11) arising from the cone, the net return is found to be

$$S_{join} = -\frac{i}{4}\tan^2\alpha\left\{2ikh - 1 + \frac{1}{2}\cot^2\alpha\sum_{n=1}^{\infty} a_n \frac{n!}{(-2ik)^{n-2}}\right\} e^{2ikh} \quad . \tag{27}$$

From this result it is obvious that we can, in principle at least, successively reduce the wavelength dependence (and hence the magnitude of the high frequency estimate) of the contribution from the join by choosing the a_n, $n = 1, 2, \ldots,$ appropriately. If all the a_n are left arbitrary, then

$$S_{join} = \frac{\pi}{2\lambda}\left\{2h\tan^2\alpha - a_1 + O(\lambda)\right\} e^{2ikh} \tag{28}$$

and the singularity is of wedge type, but if we specify

$$a_1 = 2h\tan^2\alpha \tag{29}$$

the terms $O(\lambda^{-1})$ cancel, leaving

$$S_{join} = \frac{i}{4}\left\{\tan^2\alpha - a_2 + O(\lambda)\right\} e^{2ikh} \tag{30}$$

Moreover, from (24),

$$a_o = \rho^2$$

$$a_1 = 2\rho\rho'$$

$$a_2 = \rho\rho'' + (\rho')^2$$

$$a_3 = \rho\rho'' + \frac{1}{3}\rho\rho''' \quad , \text{ etc}$$

where the primes denote differentiation with respect to z and all of the right hand sides are evaluated at the join. The above choice of a_1 therefore implies

$$\rho' = \tan\alpha$$

and gives continuity of the first derivative of the profile through the join. This is the main characteristic of the cone-sphere, and to complete the specification of this particular shape it is only necessary to demand that

$$\frac{d^2}{dz^2}(\rho^2) = -1$$

for all z, implying

$$a_2 = -1 \quad \text{and} \quad a_n = 0 \quad \text{for} \quad n > 2 \quad . \tag{31}$$

With a_1 and a_o defined by equations (29) and (25) respectively, it can be verified that the equation for the cap is the same as that used previously in the discussion of the cone-sphere, and the join contribution is as given in (17). Although its magnitude is considerably larger than the tip return for all but the very largest cone angles, its wavelength dependence is identical.

In view of the desirable effect on the join contribution produced by matching the first derivative of the profile, it is natural to consider going further and matching the second derivative also. With a_o and a_1 as given above, this additional matching requires

$$a_2 = \tan^2 \alpha \ , \tag{32}$$

which removes the leading term from (30), and reference to (27) now shows that

$$S_{join} = \frac{3\lambda}{16\pi} \left\{ a_3 + O(\lambda) \right\} e^{2ikh} \ . \tag{33}$$

At high frequencies the tip scattering then dominates regardless of a_3, and if, for convenience, we assume $a_4 = a_5 = \dots = 0$, the equation for the cap becomes

$$\rho^2 = z^2 \tan^2 \alpha + a_3 (z-h)^3 \ . \tag{34}$$

This is the so-called cubic cap whose application to the design of low cross section shapes has received some attention. We shall refer to it again in a moment.

Inasmuch as matching through the second derivative is sufficient to reduce the high frequency scattering from the join to a level below that of the tip, there is little (if anything) to be gained by attempting to match still higher derivatives. For completeness, however, we note that if

$$a_o = h^2 \tan^2 \alpha$$

$$a_1 = 2h \tan^2 \alpha$$

$$a_2 = \tan^2 \alpha$$

and

$$a_3 = a_4 = \dots a_{m-1} = 0 \ , \quad m > 3 \ ,$$

then

$$S_{join} = -\frac{i}{8} \left(\frac{i\lambda}{4\pi} \right)^{m-2} m! \left\{ a_m + O(\lambda) \right\} e^{2ikh} \ , \tag{35}$$

and the relationship between the order of the lowest non-matching derivative and the wavelength dependence of the physical optics estimate is here made explicit.

It is obvious that were this matching process continued to higher and higher derivatives, we would ultimately arrive at a 'cap' which was infinite in extent and merely the continuation of the forward cone. Attractive as it may seem, this is impractical, and even matching through the second derivative as in the cubic cap (34) leads to a substantial elongation of the basic cone-sphere shape (which is already longer than desirable for aerodynamic and systems reasons). According to physical optics, however, it is only necessary to have the cap equation (24) apply from the join to just beyond the shadow boundary. Once we are out of the illuminated region, it would seem that we can tolerate discontinuities in the derivatives of the profile, and can therefore terminate the cap more sharply, but were we to do so, the shortcomings of the physical optics method would be only too apparent. Although that part of the surface field produced by direct incident field excitation is accurately reproduced by the physical optics approximation if the surface singularity is confined to the second and/or higher derivatives of the profile, any part resulting from the reflection of energy at singularities beyond the join (or even the shadow boundary) is not taken into account; if, therefore, the body has a point at the rear, or is only slightly curved on entering the shadow and then has a wedge-type singularity, a traveling wave reflection may occur, and this could not only markedly affect the postulated current distribution in the vicinity of the join, but may also be a direct source of substantial scatter.

The difficulty is eased somewhat if wedge and point singularities are abjured, but even if we have a first derivative match throughout both the shadow and the lit regions, a surface wave reflection can still occur at places where the radius of curvature is small. If such places are not well within the shadow, any creeping wave reflected there will arrive back in the lit region with sufficient magnitude to perturb the optics field, and the more we increase the distance that these waves travel, and hence increase their decay, the greater the overall length of the body. This, then, is the dilemma that we face, and though an adequate termination can be achieved in a shorter length if the forward cone is replaced by an ogive, the reduction is not significantly greater than would have been found by increasing the cone angle to the same value as the vertex angle of the ogive.

The design of a low cross section shape which will profit from our understanding of the effect of surface singularities on the scattering is certainly not an easy task, particularly since aspects other than nose-on must be considered: a singularity well within the shadow region for nose-on incidence may be perilously close to the shadow boundary at some of the oblique angles of interest. Moreover, any serious attempt at such design requires a knowledge of the scattering superior to that afforded by physical optics alone, but it is hoped that the above discussion has given some insight into the nature of high frequency scattering, and the factors which influence it.

III
OBLIQUE INCIDENCE

The evaluation of the physical optics integral is a more involved task for oblique incidence, and the restriction to bodies of revolution no longer provides a significant amount of simplification if the direction of propagation is other than along the axis of symmetry. For back scattering, however, the general expression for the scattered field does simplify somewhat, and we note at the outset that for any metallic surface the physical optics approximation leads to a back scattered field whose polarization is that of the incident field. Only for bistatic scattering is any depolarization predicted.

This fact enables us to suppress the vector character of the field in back scattering, and if the incident electric vector is

$$\underline{E}^i = \hat{b}\, e^{i\underline{k}\cdot\underline{R}}$$

the scattered electric vector can be written as

$$\underline{E}^s = \hat{b}\,\frac{e^{ikR}}{kR}\, S$$

where the (scalar) far field amplitude S is

$$S = -\frac{2i\pi}{\lambda^2}\int_{\Sigma} \underline{k}\cdot\hat{n}\, e^{2i\underline{k}\cdot\underline{R}'}\, d\Sigma \tag{36}$$

The direction of integration is that of the propagation vector, and the integration itself is confined to the illuminated region of the surface Σ whose variable position vector is denoted by $\underline{R}'$. The upper limit of integration is the shadow boundary, i.e. the locus of the points on the body for which $\underline{k}\cdot\hat{n} = 0$, where $\hat{n}$ is the unit vector normal drawn outwards from the surface.

In the particular case of a plane wave at nose-on incidence on a body of revolution whose radius is ρ (see Fig. 1), the azimuthal integration can be carried out immediately to give the expression for S shown in equation (5), but for asymmetrical situations equation (36) is, in general, incapable of further simplification.

The first shape to which we shall apply (36) is a right circular (flat-backed) cone of half angle α and height h illuminated at an angle θ to the direction of the positive z axis. With origin of coordinates at the vertex of the cone, and notation as in Fig. 4,

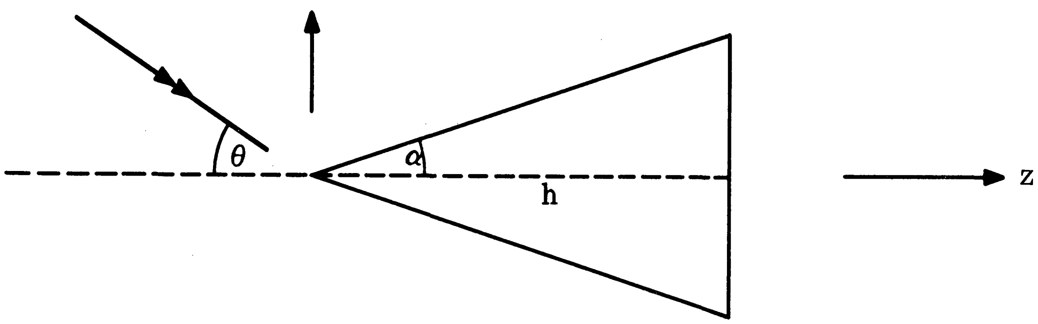

FIG. 4

$$\underline{k} \cdot \underline{R}' = \left\{ \tan\alpha \sin\theta \cos(\phi' - \phi) + \cos\theta \right\} kz' ,$$

$$\underline{k} \cdot \hat{n}\, d\sum = \left\{ \tan\alpha \quad \sin\theta \cos(\phi' - \phi) - \cos\theta \tan\alpha \right\} z'\, dz'\, d\phi' ,$$

and hence

$$S = -\frac{2i\pi}{\lambda^2} \tan\alpha \iint \left\{ \sin\theta \cos(\phi' - \phi) - \cos\theta \tan\alpha \right\} \times$$

$$\times \exp\left\{ 2ikz' \left(\tan\alpha \sin\theta \cos(\phi' - \phi) + \cos\theta \right) \right\} z'\, dz'\, d\phi' . \qquad (37)$$

If the incidence is within the backward cone ($\theta \leq \alpha$) all of the cone surface is illuminated. The above expression for S then becomes

$$S = -\frac{2i\pi}{\lambda^2}\tan\alpha\int_0^{2\pi}\int_0^h(\sin\theta\cos\phi' - \cos\theta\tan\alpha)$$

$$\cdot\exp\left\{2ikz'(\tan\alpha\sin\theta\cos\phi' + \cos\theta)\right\}z'\,dz'\,d\phi' \tag{38}$$

and the z' integration can be carried out to give

$$S = \frac{i}{8\pi}\cot\alpha\left(I_1 + e^{2ikh\cos\theta}I_2\right) \tag{39}$$

with

$$I_1 = \int_0^{2\pi}\frac{\sin\theta\cos\phi' - \cos\theta\tan\alpha}{(\sin\theta\cos\phi' + \cos\theta\cot\alpha)^2}\,d\phi' \tag{40}$$

$$I_2 = \int_0^{2\pi}\frac{\sin\theta\cos\phi' - \cos\theta\tan\alpha}{(\sin\theta\cos\phi' + \cos\theta\cot\alpha)^2}\left\{2ikh(\tan\alpha\sin\theta\cos\phi'\right.$$

$$\left.+\cos\theta) - 1\right\}\exp\left\{2ikh\tan\alpha\sin\theta\cos\phi'\right\}d\phi' \tag{41}$$

The first integral can be treated by making the substitution

$$t = \tan\frac{\phi' - \pi}{2},$$

thereby reducing the integrand to algebraic form, and from a consideration of the residues in either the upper or lower halves of the complex r plane, we have

$$I_1 = -2\pi\frac{\tan^3\alpha}{(1 - \sin^2\theta\sec^2\alpha)^{3/2}}. \tag{42}$$

As is evident from the phase factors associated with I_1 and I_2, I_1 is the contribution from the tip, and thus (Spencer, 1951),

$$S_{tip} = -\frac{i}{4}\frac{\tan^2\alpha}{(1 - \sin^2\theta\sec^2\alpha)^{3/2}}, \tag{43}$$

which is required generalization of the nose-on value (10). It is also the physical optics prediction for the far field amplitude due to an infinite cone, and since this is a body whose exact solution is known, it is appropriate to compare the two estimates. The nature of the exact solution is such that a simple expression for the scattered field is possible only for large or small cone angles. The latter is the case of most interest in the present study, and if the far field amplitude is denoted by S_V or S_H according as the displacement θ is perpendicular to, or in the plane of, the incident electric vector, the analysis in Felsen (1957) gives*

$$S_V \simeq -\frac{i}{4}\alpha^2 \frac{1-\frac{1}{4}\sin^2\theta}{\cos^3\theta} \tag{44}$$

$$S_H \simeq -\frac{i}{4}\alpha^2 \frac{1-\frac{1}{4}\sin^2\theta\,(3-\sec\theta)}{\cos^2\theta\left(\frac{1+\cos\theta}{2}\right)} \tag{45}$$

These are accurate to the first order in α^2, and if θ is also small,

$$S_V \simeq -\frac{i}{4}\alpha^2\left(1+\frac{5}{4}\theta^2\right),$$

$$S_H \simeq -\frac{i}{4}\alpha^2\left(1+\frac{3}{4}\theta^2\right)$$

Under the same approximations the physical optics answer (43) becomes

$$S_{tip} \simeq -\frac{i}{4}\alpha^2\left(1+\frac{3}{2}\theta^2\right)$$

and a comparison of these results now shows that (43) is accurate only at nose-on incidence. This is otherwise obvious from the polarization dependence of the exact returns for $\theta \neq 0$, since the physical optics estimate implies no depolarization. The expression (43) is therefore quantitatively in error for all $\theta \neq 0$, but

*The author is indebted to Dr. R E. Kleinman for the derivation of the second result from Felsen's paper.

qualitatively it does give a reasonable approximation to the off-axis scattering with either polarization. It certainly reproduces the general behavior as a function of θ, and even for θ as large as 20° its magnitude is still within (about) 10 percent of both $|S_V|$ and $|S_H|$.

The second integral, I_2, is more difficult to treat, but approximate evaluations can be achieved in two specific cases. If the incidence is so near nose-on that

$$kh \tan\alpha \sin\theta << 1 \quad , \tag{46}$$

the exponential in the integrand of (41) can be expanded and only the first two terms retained. After some algebraic manipulation we then have

$$I_2 = -\left\{1 - 2ikh\cos\theta - (2kh\cos\theta)^2\right\} I_1 - (2kh)^2 \tan\alpha\cos\theta\, I_2' + O\left\{(kh\tan\alpha\sin\theta)^2\right\}$$

where

$$I_2' = \int_0^{2\pi} \frac{\sin\theta\cos\phi' - \cos\theta\tan\alpha}{\sin\theta\cos\phi' + \cos\theta\cot\alpha}\, d\phi' \quad ,$$

and using the procedure adopted for the integral I_1, it can be shown that

$$I_2' = 2\pi\left\{1 - \frac{\cos\theta\sec^2\alpha}{\sqrt{1-\sin^2\theta\sec^2\alpha}}\right\} \quad . \tag{47}$$

Hence

$$I_2 = \left(2ikh\cos\theta - 1\right) I_1 - 2\pi(2kh)^2\tan\alpha\cos\theta \times$$

$$\times \left\{1 - \cos\theta\,\frac{1 - \sin^2\theta\sec^4\alpha}{(1-\sin^2\theta\sec^2\alpha)^{3/2}}\right\} + O\left\{(kh\tan\alpha\sin\theta)^2\right\} \tag{48}$$

and, as expected, the second group of terms on the right hand side vanishes as $\theta \longrightarrow 0$.

Apart from the multiplicative factor indicated in equation (39), I_2 is the contribution to the far field amplitude produced by the rim singularity at the base of the cone. Thus, for incidence within the backward cone and θ restricted as in (46)

$$S_{rim} \simeq -\frac{i}{4} \frac{\tan^2\alpha}{(1-\sin^2\theta\sec^2\alpha)^{3/2}} (2ikh\cos\theta - 1) e^{2ikh\cos\theta}$$

$$-i(kh)^2\cos\theta \left\{ 1 - \cos\theta \frac{1-\sin^2\theta\sec^4\alpha}{(1-\sin^2\theta\sec^2\alpha)^{3/2}} \right\} e^{2ikh\cos\theta} \tag{49}$$

and the main effect of the oblique incidence is to multiply the nose-on value (11) by the same factor as the tip return, and to change the phase appropriately. Unfortunately, this new result is also subject to the same limitations as (11), and because of the failure of physical optics to reproduce the basic features of the actual current distribution in the vicinity of a wedge singularity, equation (49) does not provide a valid approximation to the angular behavior of the rim return. Here again a more refined approach is called for.

The second case in which the integral I_2 can be treated is when the angle of incidence is such that

$$kh\tan\alpha\sin\theta >> 1 \quad , \tag{50}$$

although still confined to the backward cone. A steepest descents evaluation of the integral (41) is then appropriate, and if we first make the substitution $\phi' = \phi'' + \pi$, we have

$$I_2 \sim -2\pi\tan\alpha \frac{\sin\alpha\sin(\alpha+\theta)}{\cos^2(\alpha+\theta)} \left\{ 2ikh\sec\alpha\cos(\alpha+\theta) - 1 \right\} \times$$

$$\times J_0(2kh\tan\alpha\sin\theta) \tag{51}$$

where J_0 is the zeroth order Bessel function of the first kind. The corresponding rim return is, from (39),

$$S_{rim} \sim -\frac{i}{4}\,\frac{\sin\alpha\sin(\alpha+\theta)}{\cos^2(\alpha+\theta)}\left\{2ikh\sec\alpha\cos(\alpha+\theta)-1\right\} J_o(2kh\tan\alpha\sin\theta)e^{2ikh\cos\theta} \tag{52}$$

and notwithstanding the condition (50) under which it was derived, the result goes over into the nose-on value (11) when $\theta = 0$. If, on the other hand, we apply (50) more uniformly, then

$$S_{rim} \sim \frac{\pi h}{\lambda}\tan\alpha\tan(\alpha+\theta)\; J_o(2kh\tan\alpha\sin\theta)e^{2ikh\cos\theta}\,, \tag{53}$$

which is the anlogue of the nose-on expression (12), and if we further replace the Bessel function by the leading term of its asymptotic expansion for large argument,

$$S_{rim} \sim \sqrt{\frac{h\tan\alpha}{2\lambda\sin\theta}}\tan(\alpha+\theta)\cos\left(2kh\tan\alpha\sin\theta-\frac{\pi}{4}\right)e^{2ikh\cos\theta} \tag{54}$$

This can be written alternatively as

$$S_{rim} \sim \frac{1}{2}\sqrt{\frac{h\tan\alpha}{2\lambda\sin\theta}}\tan(\alpha+\theta)\left\{e^{2ikh\sec\alpha\cos(\alpha+\theta)+i\frac{\pi}{4}}+e^{2ikh\sec\alpha\cos(\alpha-\theta)-i\frac{\pi}{4}}\right\} \tag{55}$$

and reference to Fig. 5 now shows that the rim return is made up of contributions from the extreme points of the base, which contributions differ only in phase. The

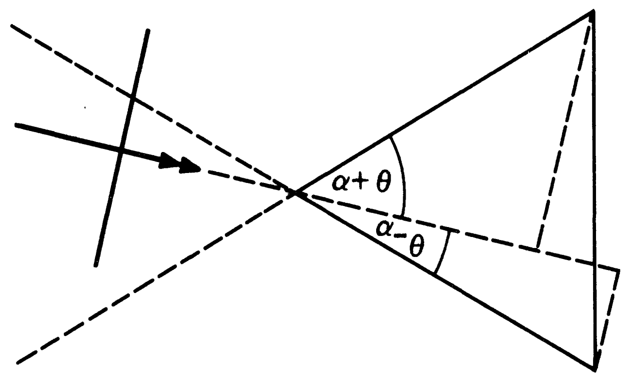

FIG. 5

physical reason for requiring that the angle of incidence be within the backward cone is evident from (55), and it is natural to expect that if this condition were violated, the shadowing produced by the cone would remove the contribution attributable to the most distant point of the rim. In contrast, as θ approaches zero all points of the rim will contribute equally, and the requirement that θ be bounded away from zero is also evident from the above interpretation of S_{rim}. The mathematical representation of this focussing effect near $\theta = 0$ is provided by the Bessel function J_o (see equations 52 and 53).

Before leaving this discussion of the right circular cone for $\theta \leq \alpha$, it is desirable to point out a further restriction common to the evaluations of both I_1 and I_2. For cones with angle $\alpha < \pi/4$ the direction $\theta = \pi/2 - \alpha$ of the specular flash lies outside the backward cone, but if $\alpha > \pi/4$ the condition $\theta \leq \alpha$ is no longer sufficient to exclude the specular direction. Although such cones are not of direct interest in the present study, it will be observed that the expressions which we have derived for S_{tip} (equation 43) and S_{rim} (equations 49 and 52 through 54) are all infinite when $\theta = \pi/2 - \alpha$. This is due to the vanishing of the exponent in the integrand of (38) for $\phi' = \pi$ and $\theta = \pi/2 - \alpha$, and the consequent creation of a pole in both I_1 and I_2 when the z' integration is carried out by parts. The exclusion of the specular direction is therefore necessary, and if $\alpha > \pi/4$ this is a restriction additional to those previously imposed.

In spite of the simple and straight forward nature of the expression for S given in equation (38), it has not proved possible to evaluate the integrals analytically in such a way as to be valid for both the specular and nose-on directions, and rather than discuss separately the special case of the specular flash for $\alpha > \pi/4$, it is convenient to include it as part of a general treatment of oblique incidence.

For angles outside the backward cone only a portion of the surface is illuminated, and if θ is such that $\alpha < \theta < \pi/2$ so that the base of the cone is still shadowed, the far field amplitude is given by (37) with

$$\pi + \phi - f(z') < \phi' < \pi + \phi - f(z')$$

and $0 \leq z' \leq h$, where $f(z')$ specifies the location of the shadow boundary. A precise evaluation of the expression for S is now almost impossible to achieve, but by application of the steepest descents method to the ϕ' integral, the complication presented by the variable limits of integration is in large measure avoided. On the assumption that the main contribution to the z' integral is provided by those z' for which $2kz' \tan\alpha \sin\theta >> 1$, the saddle point is $\phi' = \pi + \phi$, and

$$S = -e^{-i\frac{\pi}{4}} k\sqrt{\frac{\tan\alpha}{2\lambda \sin\theta}} \sec\alpha \sin(\alpha+\theta) \int_0^h e^{2ikz' \sec\alpha \cos(\alpha+\theta)} \sqrt{z'}\, dz' ,$$

which can be written as

$$S = \frac{1}{2} e^{i\frac{\pi}{4}} \sqrt{\frac{h\tan\alpha}{2\lambda \sin\theta}} \tan(\alpha+\theta)\, e^{2ikh \sec\alpha \cos(\alpha+\theta)} \times$$

$$\times \left\{ 1 - \mathfrak{F}\left(\sqrt{2kh \sec\alpha \cos(\alpha+\theta)} \right) \right\} \tag{56}$$

where

$$\mathfrak{F}(x) = \frac{e^{-ix^2}}{x} \int_0^x e^{it^2}\, dt$$

and is related to the Fresnel integral (see, for example, Jahnke and Emde, 1945).

For $x >> 1$, $\mathfrak{F}(x) = O(x^{-1})$ and the function can be neglected in comparison with the first term in (56), in which case

$$S = \frac{1}{2} e^{i\frac{\pi}{4}} \sqrt{\frac{h\tan\alpha}{2\lambda \sin\theta}} \tan(\alpha+\theta)\, e^{2ikh \sec\alpha \cos(\alpha+\theta)} \quad . \tag{57}$$

This represents the return in the far side lobes of the specular flash, and the phase is that appropriate to a contribution from the base end of the nearest generator of the cone. As such the far field amplitude is identical to the expression for S_{rim} given in equation (55) apart from the omission of the contribution from the most distant point of the base. Since $\theta > \alpha$, this point is, of course, shadowed.

If x is small compared with unity,

$$\mathfrak{T}(x) = 1 - \frac{2}{3} ix^2 + O(x^4)$$

and consequently, as θ approaches $\pi/2 - \alpha$, the far field amplitude reduces to

$$S = -\frac{kh}{3} e^{-i\frac{\pi}{4}} \sqrt{\frac{kh \sin\alpha}{\pi}} \sec^2 \alpha \quad . \tag{58}$$

This is the specular contribution. It is equivalent to the broadside return from a thick cylinder whose length is the slant length, $h \sec\alpha$, of the cone and whose radius is $\frac{4}{9}$ $a \sec\alpha$, where $a = h \tan\alpha$ is the base radius of the cone, but this choice of dimensions is not unique, nor is it sufficient for computing the side lobes. Indeed, the far side lobes must be calculated from equation (57), and to investigate the transition from (57) to (58) it is necessary to determine S from (56) using the available tabulations of the Fresnel integral. The asymmetrical nature of the side lobes about the direction $\theta = \pi/2 - \alpha$ is then apparent, and can also be seen from equation (56) if the function $\mathfrak{T}$ is approximated by its small argument expansion. The net effect is to broaden the scattering pattern (including the main lobe) for $\theta > \pi/2 - \alpha$, and the weighting of energy in favor of aspects beyond the specular direction is evident in the experimental data of Keys and Primich (1959 a, b).

In the specular direction itself the cross section is, from (58),

$$\sigma = \frac{4}{9} kh^3 \sin\alpha \sec^4 \alpha$$

which can be written as

$$\frac{\sigma}{\lambda^2} = K(ka)^3 \tag{59}$$

where a is, as before, the base radius of the cone and

$$K = \frac{\operatorname{cosec}^2 \alpha \sec \alpha}{9\pi^2} \tag{60}$$

Inasmuch as K is a function of α alone, equation (58) is quite convenient, and the behavior of the parameter K is shown in Fig. 6. As α increases from zero, K decreases rapidly, passing through the value unity when $\alpha = 6.1^o$ (approx.) and dropping to a shallow minimum at $\alpha = \tan^{-1}\sqrt{2}$ ($\simeq 54.7^o$) where K = 0.0295. Thereafter K increases slowly.

From Fig. 6 it is a simple matter to determine the specular return for any ka and α, but because of the practical importance of the scattering in this direction it is desirable to have some feel for the accuracy of the prediction. This we can obtain by comparison with the above-mentioned experimental data. Using 14 separate models with ka values spanning the range $0.933 \leq ka \leq 9.02$ for each of the half-cone angles $\alpha = 4^o, 7.5^o, 9.6^o, 12^o, 15^o$ and 20^o, Keys and Primich (1959a) measured the complete back scattering patterns for both vertical and horizontal polarizations. Similar data for $\alpha = 30^o, 37.5^o, 45^o, 52.5^o$ and 60^o was presented in a subsequent report (Keys and Primich, 1959b) and taking just the values of the cross section in the specular direction, graphs such as those in Fig. 7 can be constructed. Each point is the average of the measured values of σ/λ^2 for the flashes from the left and right hand sides of the cone, and the theoretical curves are based on equation (59). All in all the agreement is good, particularly for the larger ka, and though there is some scatter to the points, the general trend is well predicted by the theoretical expression. The maximum discrepancy for ka $\geq$ 3 is no more than 3 db. This is attained only at one or two points and is somewhat larger than the stated accuracy of the measured data ($\pm$ 2 db), but the reading of values from the small graphs contained in the reports could account for the

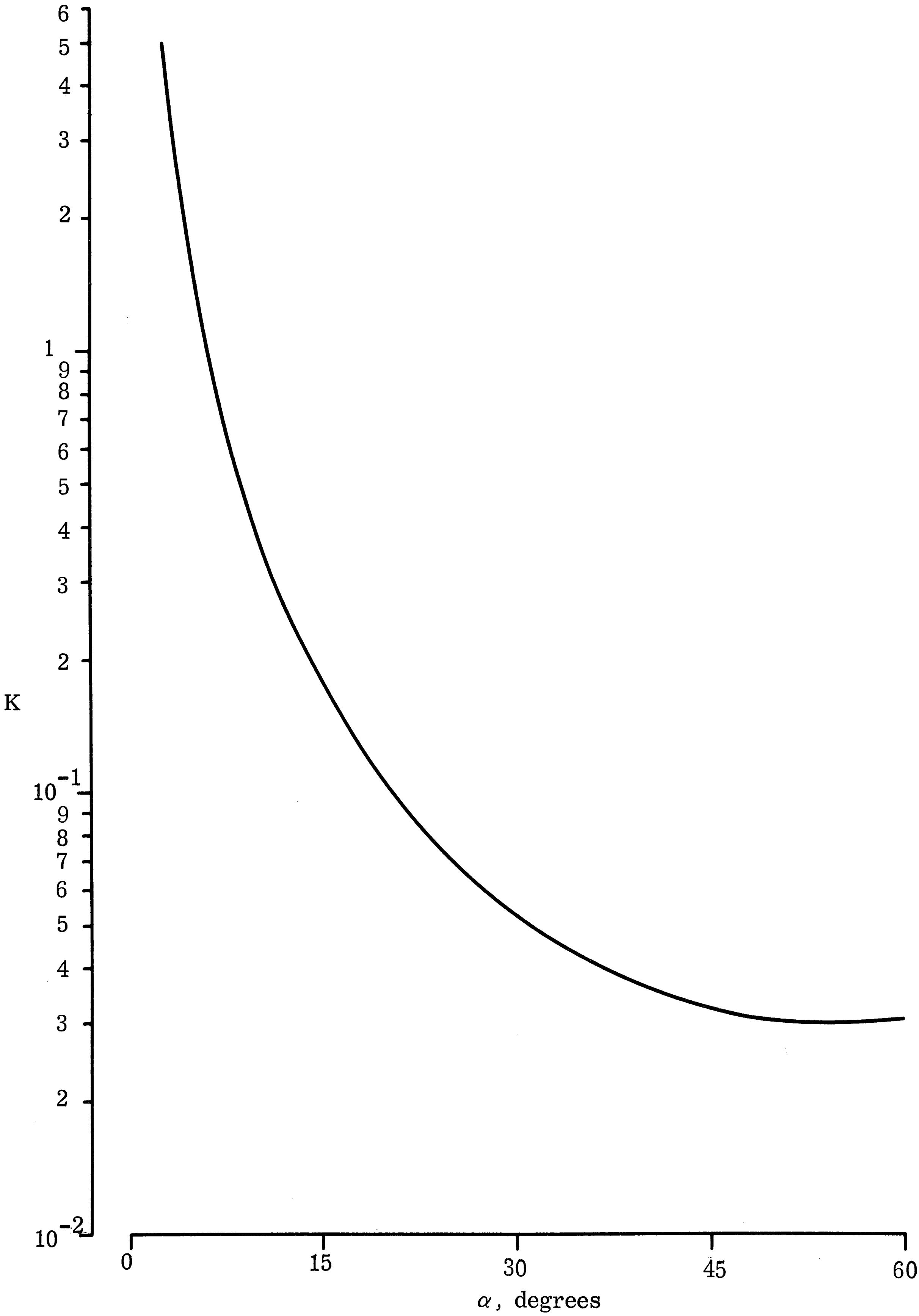

FIG. 6: PARAMETER K (SEE EQUATIONS 59 AND 60) AS FUNCTION OF α.

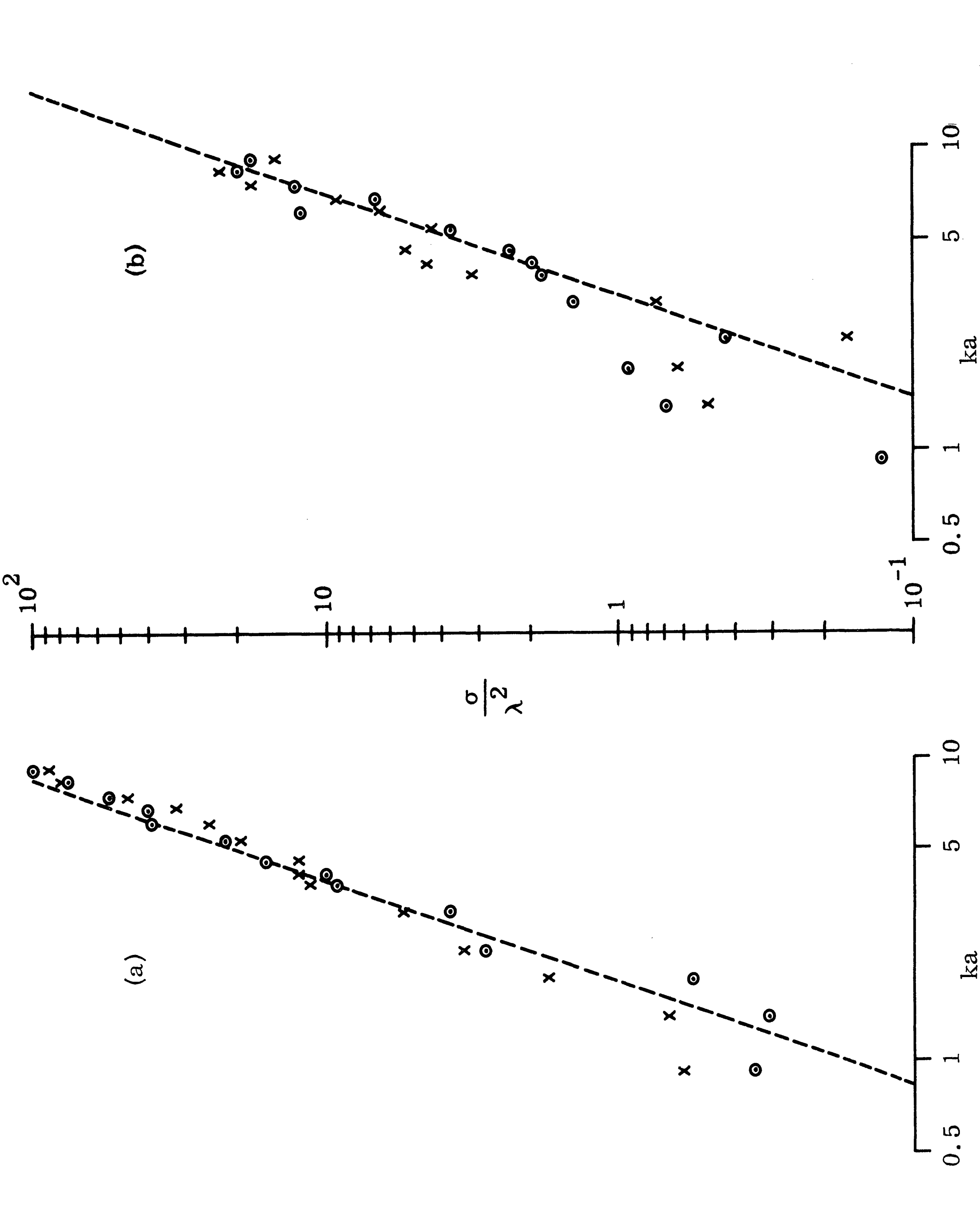

FIG. 7: SPECULAR FLASH CROSS SECTION FOR FLAT-BACKED CONE WITH (a) $\alpha = 15^o$ AND (b) $\alpha = 60^o$: (xxx) Experimental, Horizontal Polarization; (⊙⊙⊙) Experimental, Vertical Polarization; (---) Theoretical, equation (59).

difference. Moreover, if $ka \geq 3$ the <u>average</u> discrepancy between theory and experiment is more nearly 1 db.

For $ka < 3$, however, the formula under-estimates the magnitude of the flash to an extent which increases with decreasing ka, and this is particularly noticeable for the larger α. One reason for this is at once obvious on examining the measured scattering patterns: as ka decreases with α constant, the nose-on lobe increases in width whilst the magnitude of the specular flash decreases, ultimately becoming swamped by the skirts of the frontal lobe. With $\alpha = 60^o$, for example, there is no evidence of the flash until ka has reached 2.33 (horizontal polarization) or 5.31 (vertical polarization), and though the flash emerges sooner when α is smaller, it would still seem necessary that the slant length be of order λ or greater for the optics approximation to have any real validity. This in turn implies $ka > 2\pi \sin\alpha$, and the lower bound is not inconsistent with the value of ka at which the specular return emerges for the smaller angle cones.

A complete comparison of the experimental and theoretical values of σ/λ^2 at $\theta = \pi/2 - \alpha$ is presented in Figs. 8a through 8k in which the ratios $\sigma_{exp}/\sigma_{theor}$, in db, are plotted as functions of ka for the various cone angles. Several features are apparent. For the larger values of ka and $\alpha \geq 20^o$, the theoretical formula provides a reasonable approximation to the experimental data, and though there is a fair amount of scatter to the points, the scatter is about the theoretical value. If $\alpha < 20^o$, however, the differences are more marked, and the formula now over-estimates the data to an extent which increases with decreasing α, being of order 2 db for $\alpha = 12^o$, rising to about 5 db for $\alpha = 4^o$. We note that most of the systematic discrepancy is removed if the theoretical expression for σ is multiplied by a factor of the form

$$1 - e^{-6\alpha} \qquad (61)$$

where α is in radians.

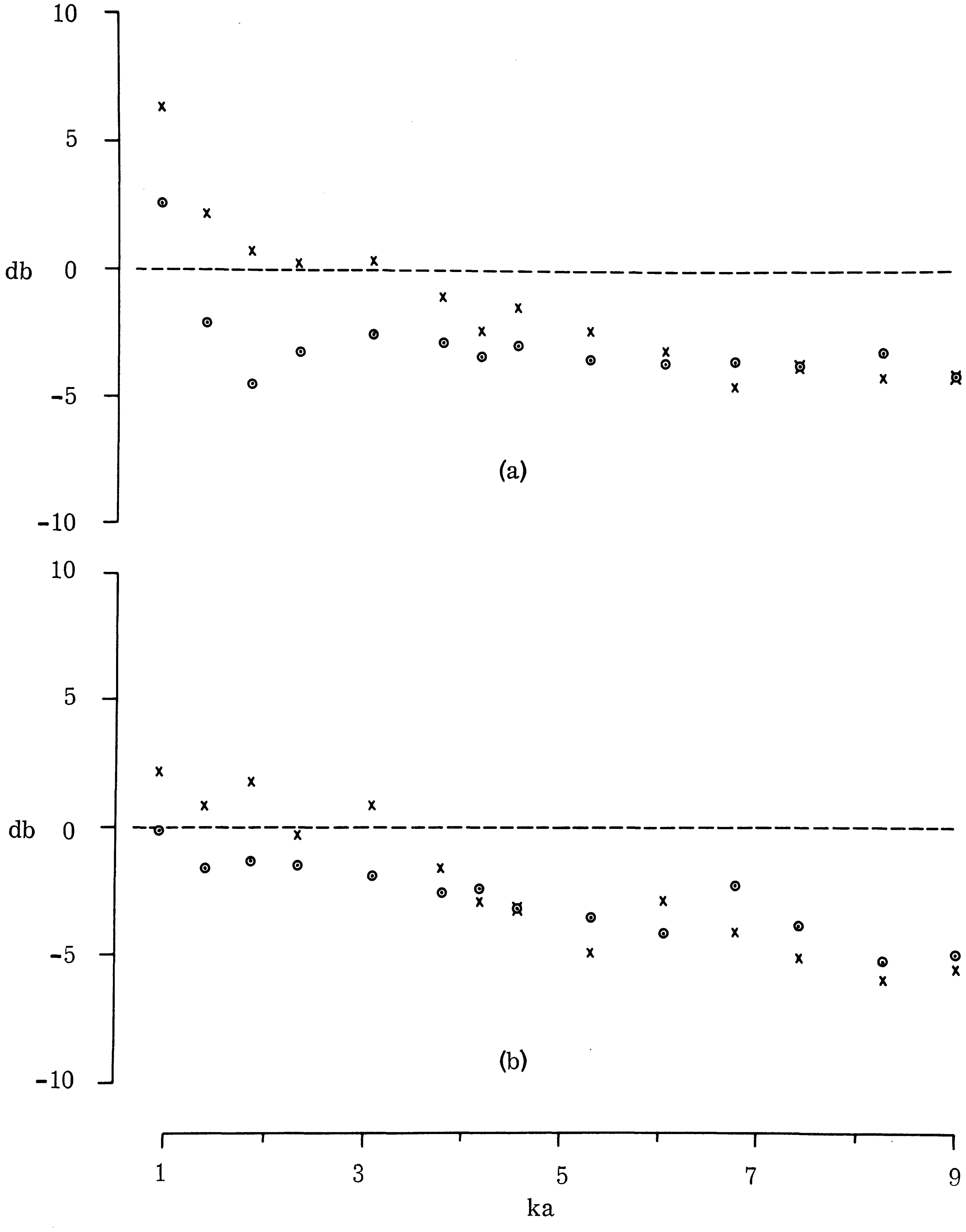

FIG. 8a, b: RATIO OF EXPERIMENTAL TO THEORETICAL SPECULAR FLASH CROSS SECTION FOR FLAT-BACKED CONES WITH (a) $\alpha = 4^{o}$ AND (b) $\alpha = 7\,1/2^{o}$: (xxx) Horizontal Polarization, (⊙⊙⊙) Vertical Polarization.

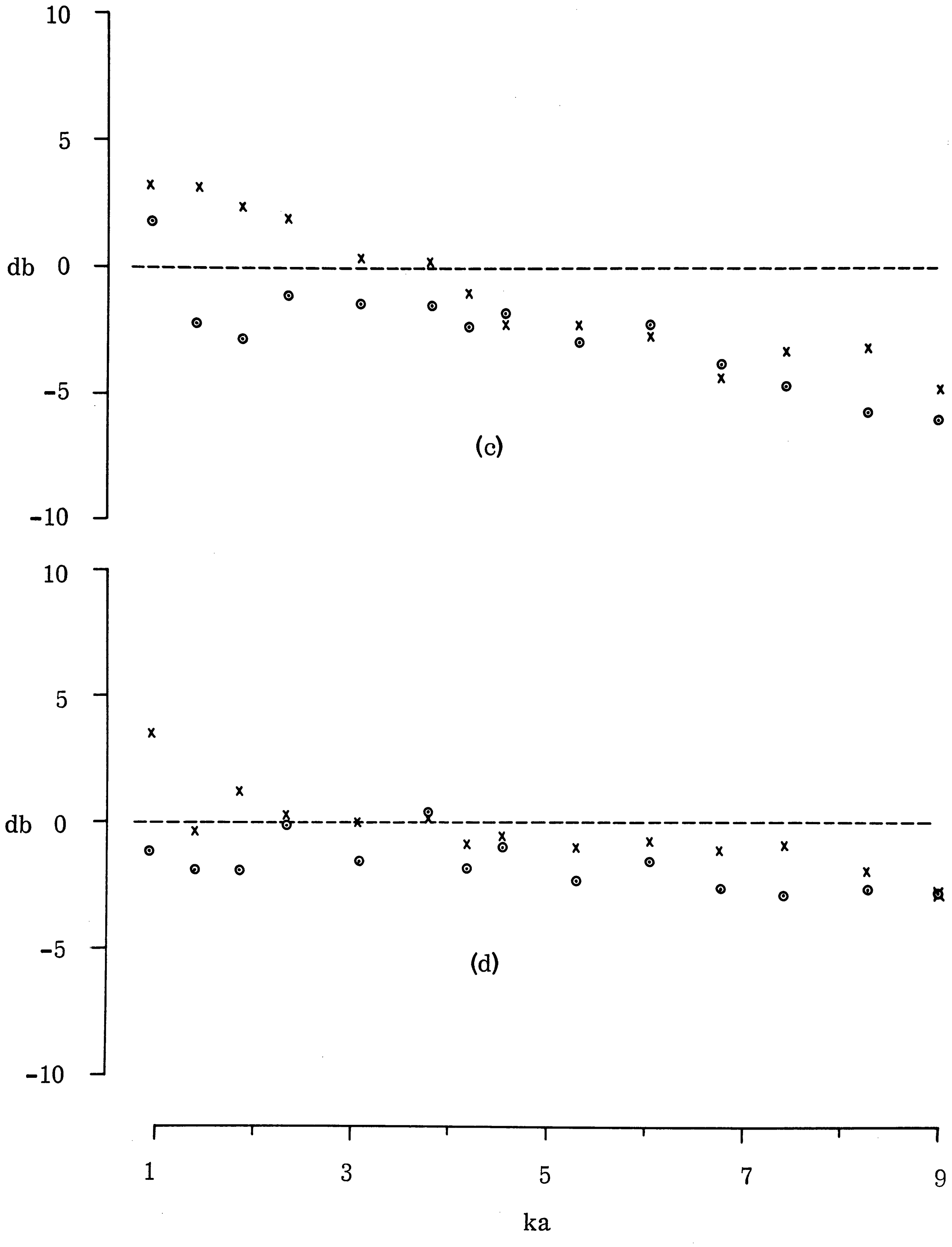

FIG. 8c, d: RATIO OF EXPERIMENTAL TO THEORETICAL SPECULAR FLASH CROSS SECTION FOR FLAT-BACKED CONES WITH (c) $\alpha = 9.6^{o}$ AND (d) $\alpha = 12^{o}$: (xxx) Horizontal Polarization, (ooo) Vertical Polarization.

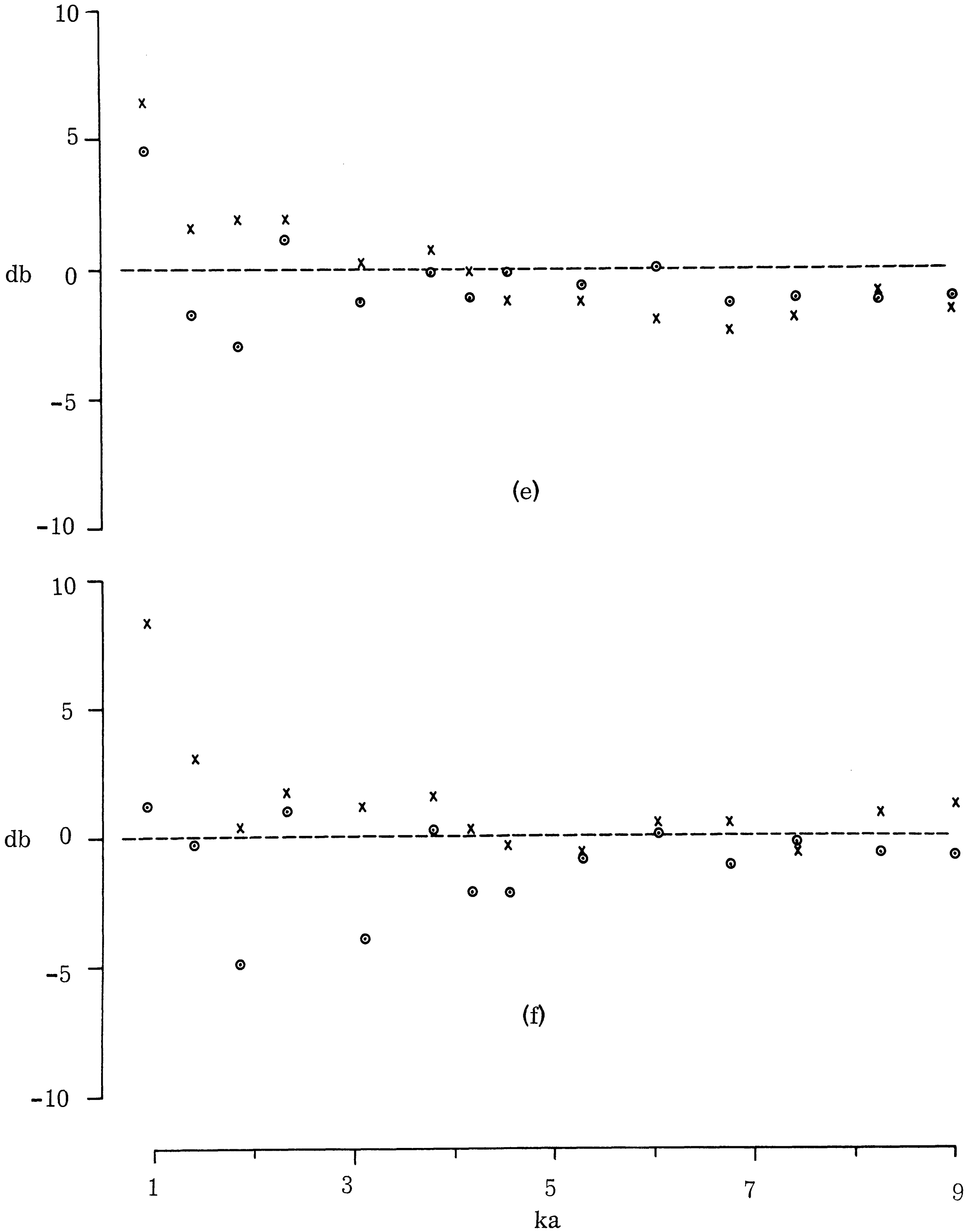

FIG. 8e, f: RATIO OF EXPERIMENTAL TO THEORETICAL SPECULAR FLASH CROSS SECTION FOR FLAT-BACKED CONES WITH (e) $\alpha = 15^{o}$ AND (f) $\alpha = 20^{o}$: (xxx) Horizontal Polarization, (⊙⊙⊙) Vertical Polarization.

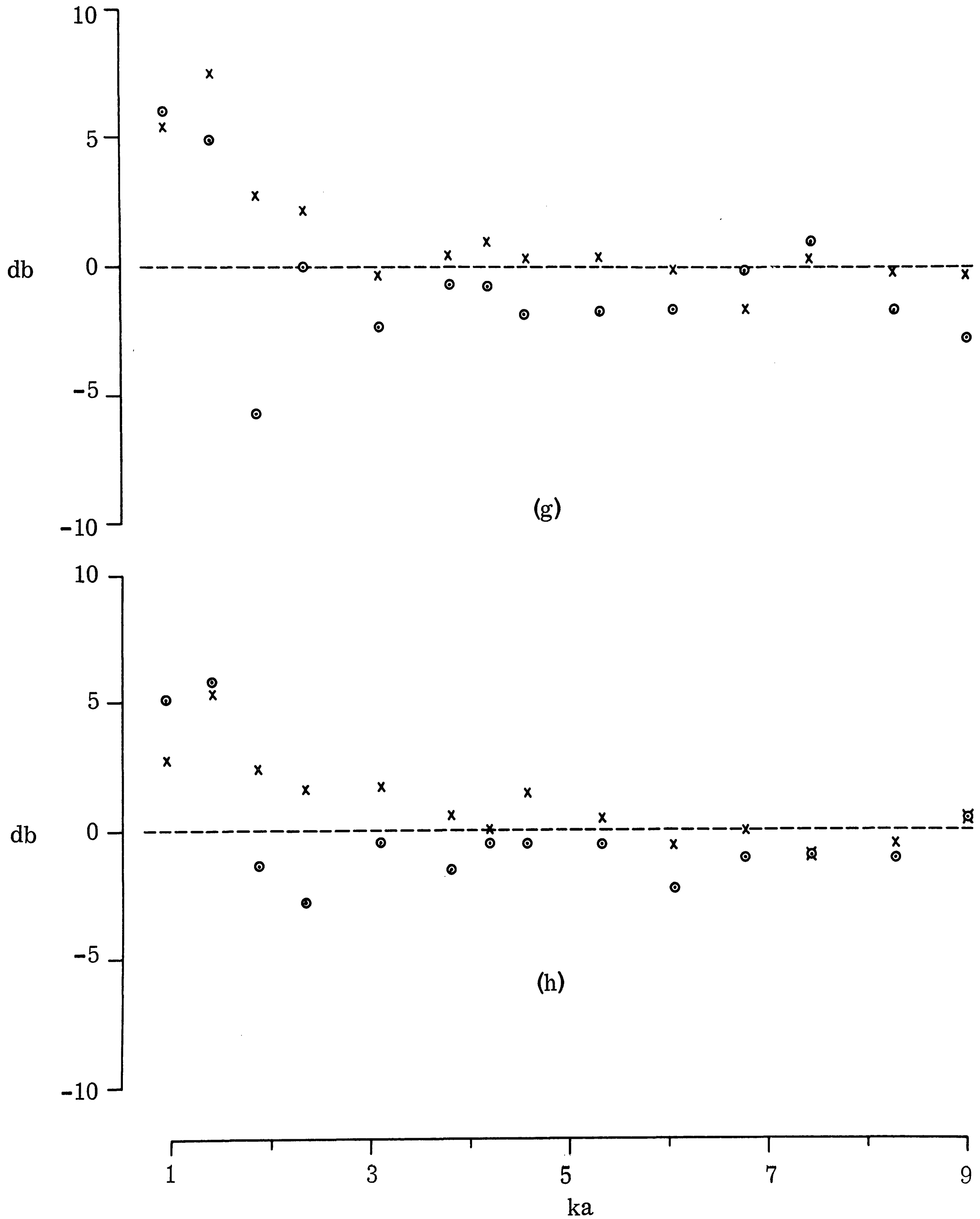

FIG. 8g, h: RATIO OF EXPERIMENTAL TO THEORETICAL SPECULAR FLASH CROSS SECTION FOR FLAT-BACKED CONES WITH (g) $\alpha = 30^{o}$ AND (h) $\alpha = 37\,1/2^{o}$: (xxx) Horizontal Polarization, (⊙⊙⊙) Vertical Polarization.

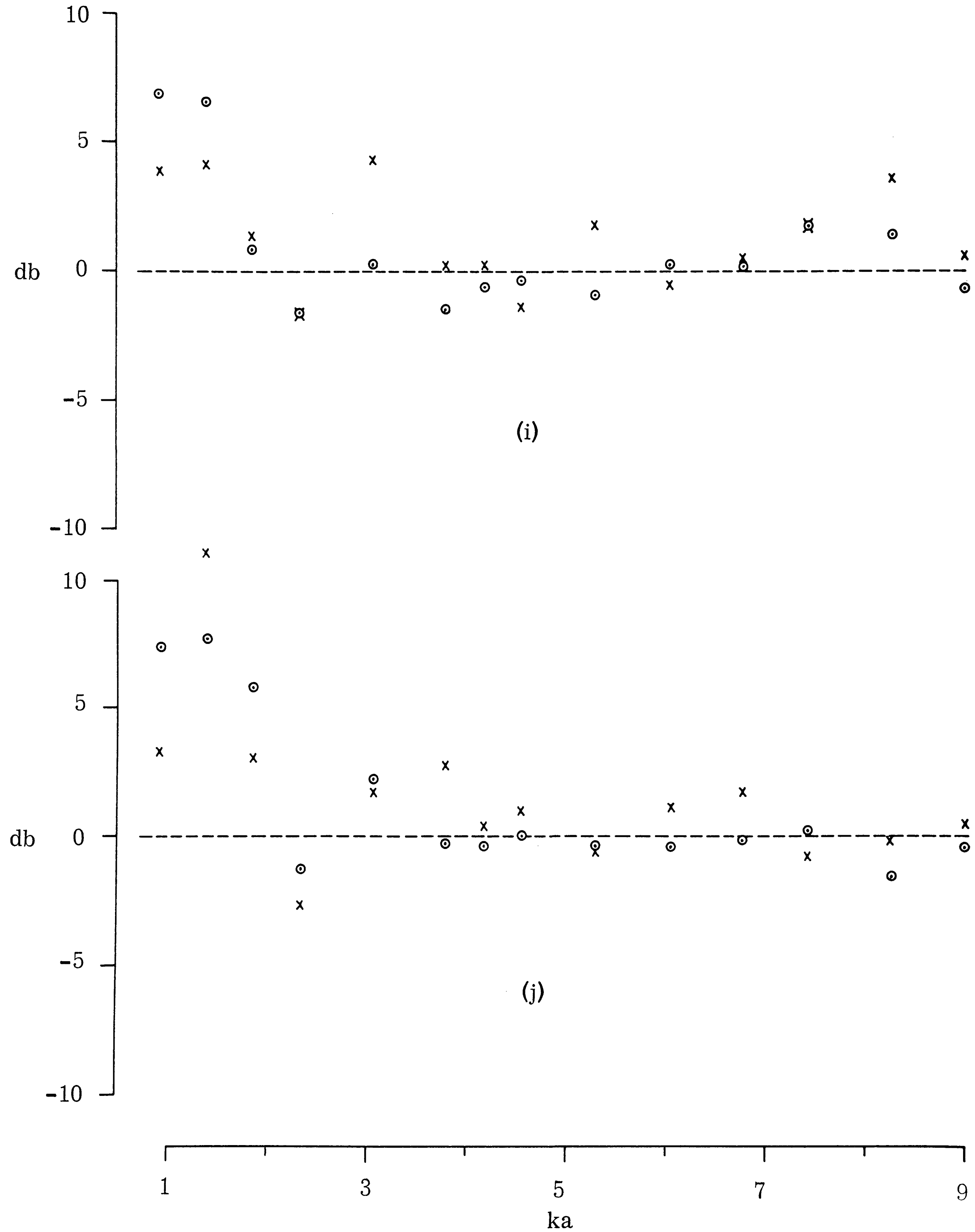

FIG. 8 i, j: RATIO OF EXPERIMENTAL TO THEORETICAL SPECULAR FLASH CROSS SECTION FOR FLAT-BACKED CONES WITH (i) $\alpha = 45^{\circ}$ AND (j) $\alpha = 52\frac{1}{2}^{\circ}$: (xxx) Horizontal Polarization, (⊙⊙⊙) Vertical Polarization.

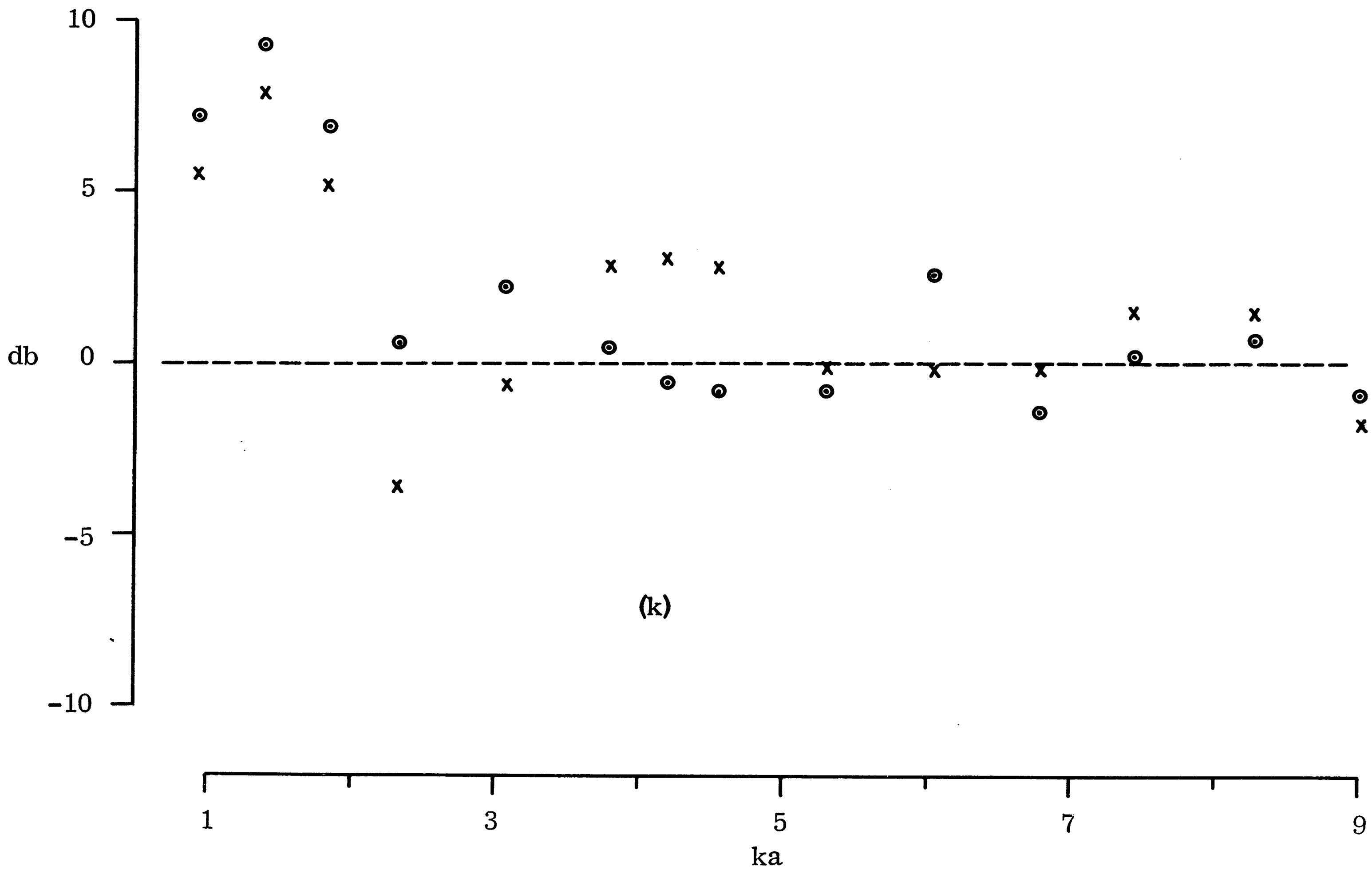

FIG. 8k: RATIO OF EXPERIMENTAL TO THEORETICAL SPECULAR FLASH CROSS SECTION FOR FLAT-BACKED CONES WITH (k) $\alpha = 60^{\circ}$: (xxx) Horizontal Polarization, (⊙⊙⊙) Vertical Polarization.

For ka ≥ 3 there is no obvious polarization dependence to the scattering, but if ka is less than (about) 3, the horizontally polarized return tends to exceed the vertically polarized one by 2 or more db. This is consistent with the polarizing properties of a thin cylinder. If ka < 1, theory underestimates the measured data, and does so for a somewhat more extended range of ka if α is large (up to and beyond ka = 2 if $\alpha = 60^{o}$). The probable cause is the relatively small slant length of the cone, and the resonant type of current distribution that then occurs, but the submersion of the specular return beneath the nose-on lobe is also a factor for the larger cone angles.

In the light of this comparison it is concluded that the physical optics formula (59) is a valid approximation to the actual specular return from the sides of a right-angled cone for $\alpha \geq 20^{o}$, and if ka ≥ 3 the average discrepancy between theory and experiment is no more than (about) 1 db. If, on the other hand, the formula is multiplied by the strictly-empirical factor (61) to give

$$\frac{\sigma}{\lambda^2} = K(ka)^3 (1 - e^{-6\alpha}) \tag{62}$$

the restriction on α is removed, and the resulting estimate would appear accurate to within (about) 2 db for all ka ≥ 2.

For angles of incidence greater than $\pi/2$ the base of the cone is no longer shadowed and the expression (37) for the far field amplitude is changed accordingly. Such angles are, however, of little interest in the present study, and rather than pursue this investigation of the flat-backed cone any further, we shall now explore the effects of other terminations.

Consider, therefore, the body shown in Fig. 3, consisting of a cone terminated in a sphere with an angular discontinuity δ between the tangents to the cone and sphere at the join. When the angle of incidence is within the backward cone, i.e. $\theta \leq \alpha$, all of the cone surface is illuminated, and the far field amplitude in the back scattering direction differs from that given in equation (38) (and henceforth denoted by S^{cone}) if any of the cap is visible. The condition for this is

$$X \geq h(1 - \tan\alpha \tan\theta) \quad ,$$

which is equivalent to

$$\delta \geq -\alpha - \theta$$

(see Fig. 3), and from equation (36) the additive contribution to the far field amplitude associated with the cap is

$$S^{cap} = -\frac{2i\pi}{\lambda^2} b^2 e^{2ikX\cos\theta} \int_0^{2\pi} \int_{\frac{\pi}{2}-(\alpha+\delta)}^{\gamma} (\sin\theta \sin\theta' \cos\phi' - \cos\theta \cos\theta') \times$$

$$\times \exp\left\{ 2ikb(\sin\theta \sin\theta' \cos\phi' - \cos\theta\cos\theta')\right\} \sin\theta' \, d\theta' \, d\phi \qquad (63)$$

where

$$b = \left\{ (h\tan\alpha)^2 + (X-h)^2 \right\}^{1/2} \qquad (64)$$

is the radius of the cap and $\gamma = \gamma(\phi')$ is the value of θ' corresponding to the shadow boundary.

A precise evaluation of the integrals in (63) would be difficult to achieve, but since the physical optics estimate of the shadow boundary effect is known to be in error, there is no point in attempting its calculation. We shall therefore ignore the contribution provided by the upper limit γ of the θ' integration. In contrast, the lower limit gives rise to the join contribution of the cap. This is of interest, and if we assume that

$$\sin\theta \cos\theta' \cos\phi' + \cos\theta \sin\theta' \neq 0 \qquad (65)$$

throughout the entire ranges of the θ' and ϕ' integrations, thereby ruling out the possibility of any specular return from the cap at this aspect, we can write

$$S_{join}^{cap} = -\frac{2i\pi}{\lambda^2} b^2 e^{2ikX\cos\theta} \int_0^{2\pi} \int_{\frac{\pi}{2}-(\alpha+\delta)} (\sin\theta \sin\theta' \cos\phi' - \cos\theta\cos\theta') \times$$

$$\times \exp\left\{2ikb(\sin\theta\sin\theta' \cos\phi - \cos\theta\cos\theta')\right\} \sin\theta' \, d\theta' \, d\phi' \qquad (66)$$

where the absence of the upper limit indicates that the θ' integral is evaluated only at the lower limit, $\theta' = \frac{\pi}{2} - (\alpha+\delta)$. It is now a straight forward matter to obtain an asymptotic evaluation of the integral.

Since the θ' derivative of the exponent is, by assumption, non-vanishing in the range, successive integrations by parts give

$$\int_{\frac{\pi}{2}-(\alpha+\delta)} (\sin\theta\sin\theta' \cos\phi' - \cos\theta\cos\theta')\exp\left\{2ikb(\sin\theta\sin\theta' \cos\phi' - \cos\theta\cos\theta')\right\}\sin\theta' d\theta'$$

$$= \frac{\cot(\alpha+\delta)}{(2kb)^2} \cdot \frac{e^{2ik(h-X)\cos\theta + 2ikh\tan\alpha\sin\theta\cos\phi'}}{\sin\theta\cos\phi' + \cos\theta\cot(\alpha+\delta)} \times$$

$$\times\left\{2ikh\tan\alpha(\sin\theta\cos\phi' - \cos\theta\tan(\alpha+\delta)) - \frac{\sin\theta\cos\phi' - \cos\theta\tan(\alpha+\delta)}{\sin\theta\cos\phi' + \cos\theta\cot(\alpha+\delta)} - \frac{\mathrm{cosec}^2(\alpha+\delta)(1-\sin^2\theta\sin^2\phi')}{(\sin\theta\cos\phi' + \cos\theta\cot(\alpha+\delta))^2} + O\left(\frac{1}{kh}\right)\right\}$$

which simplifies somewhat the expression S_{join}^{cap}. For the cone by itself the join contribution is, from (39),

$$S_{join}^{cone} = \frac{i}{8\pi} \cot\alpha \, e^{2ikh\cos\theta} I_2$$

where I_2 is given in equation (41), and hence, by adding the separate effects of the cap and cone, the net far field amplitude associated with the join is

$$S_{join} = \frac{i}{8\pi} e^{2ikh\cos\theta} \int_0^{2\pi} \left\{ 2ikh \tan\alpha \, P + Q + O\left(\frac{1}{kh}\right) \right\} \times$$

$$\times \exp\left\{ 2ikh \tan\alpha \sin\theta \cos\phi' \right\} d\phi' \tag{67}$$

with

$$P = \frac{(\cot\alpha - \cot(\alpha+\delta))(1 - \sin^2\theta \sin^2\phi')}{(\sin\theta\cos\phi' + \cos\theta\cot\alpha)(\sin\theta\cos\phi' + \cos\theta\cot(\alpha+\delta))} , \tag{68}$$

$$Q = -\frac{(\cot\alpha - \cot(\alpha+\delta))}{(\sin\theta\cos\phi' + \cos\theta\cot\alpha)^2(\sin\theta\cos\phi' + \cos\theta\cot(\alpha+\delta))^2} \times$$

$$\times \left\{ \sin^3\theta\cos^3\phi' + \sin\theta\cos^2\theta\cos\phi'(2 + \cot\alpha\cot(\alpha+\delta)) \right.$$

$$\left. + \cos^3\theta(\cot\alpha + \cot(\alpha+\delta)) \right\}$$

$$+ \frac{\cot(\alpha+\delta)\,\mathrm{cosec}^2(\alpha+\delta)\,(1 - \sin^2\theta\sin^2\phi')}{(\sin\theta\cos\phi' + \cos\theta\cot(\alpha+\delta))^3} . \tag{69}$$

Comparing this with equation (16) and noting that the expressions for S_{join} are of the same form, we see at once that a wedge-like join is not a more significant contributor at oblique angles of incidence than at nose-on. Indeed, for $\theta = 0$ the expressions for P and Q become

$$\tan(\alpha+\delta) - \tan\alpha \quad \text{and} \quad \sec^2\alpha$$

respectively. The integrand of (67) is then independent of ϕ', and since

$$b\sin(\alpha+\delta) = X - h \quad , \quad b\cos(\alpha+\delta) = h\tan\alpha \quad ,$$

S_{join} reduces to that given in equation (16).

The improvement in the high frequency response of the join obtained at nose-on incidence by smoothly joining the cap to the cone also occurs at oblique incidence, and on putting $\delta = 0$ in (68) and (69) we have

$$P = 0$$

$$Q = \frac{\cot\alpha \operatorname{cosec}^2\alpha (1 - \sin^2\theta \sin^2\phi')}{(\sin\theta\cos\phi' + \cos\theta\cot\alpha)^3} \quad .$$

Thus, for a cone-sphere,

$$S_{join} = \frac{i}{8\pi}\sec^2\alpha\, e^{2ikh\cos\theta}\int_0^{2\pi}\frac{1 - \sin^2\theta\sin^2\phi'}{(\sin\theta\cos\phi' + \cos\theta\cot\alpha)^3}\times$$

$$\times \exp\left\{2ikh\tan\alpha\sin\theta\cos\phi'\right\} d\phi' + O\left(\frac{1}{kh}\right) \qquad (70)$$

and though a precise evaluation of the integral is not possible if $\theta \neq 0$, by writing (70) as

$$S_{join} = \frac{i}{4\pi}\sec^2\alpha e^{2ikh\cos\theta}\int_{-1}^{1}\frac{\cos^2\theta + x^2\sin^2\theta}{(\cos\theta + x\tan\alpha\sin\theta)^3}\times$$

$$\times\ e^{2ikhx\tan\alpha\sin\theta}\frac{dx}{(1-x^2)^{1/2}} + O\left(\frac{1}{kh}\right)$$

and assuming

$$kh\tan\alpha\sin\theta >> 1$$

the asymptotic theory of Erdélyi (1956, pp 49 and 50) can be applied to give (Ruehr, 1963):

$$S_{join} \sim \frac{i}{8}\sec^2\alpha e^{2ikh\cos\theta}\left\{\frac{\cos^3\alpha}{\cos^3(\alpha-\theta)}H_o^{(1)}(2kh\tan\alpha\sin\theta)\right.$$

$$\left. + \frac{\cos^3\alpha}{\cos^3(\alpha+\theta)}H_o^{(2)}(2kh\tan\alpha\sin\theta)\right\} . \qquad (71)$$

This is finite at $\theta = 0$ and in agreement with (16) there in spite of the formal restriction to angles away from zero. Moreover, for small θ ($kh \tan\alpha \sin\theta << 1$), equation (71) can be approximated as

$$S_{join} \sim \frac{i}{4} \sec^2 \alpha \, e^{2ikh \cos\theta} J_o(2kh \tan\alpha \sin\theta) \tag{72}$$

which can be confirmed by a small angle expansion applied directly to (70). The appearance of the Bessel function J_o is typical of the return from a ring or a disc.

Using the expression for S_{join} in (71), the cross section σ/λ^2 attributable to the cone-sphere join has been computed for $\alpha = 12\,1/2^o$ and $kh \tan\alpha = 3, 10$, and in Fig. 9 the results are plotted as functions of θ, $0 \leq \theta \leq \alpha$. Although the width of the scattering lobe is not determined by the radius $kh \tan\alpha$ of the ring singularity alone, it in general decreases as this increases, and for the larger of the two radii considered the first minimum occurs within the backward cone. On the other hand, for small angle cones the numerical differences between the expressions for S_{join} given in equations (71) and (72) are relatively insignificant. In this case, the width is almost exclusively determined by the value of $kh \tan\alpha$, and for kh sufficiently large, the total width measured at the -3 db level is approximately

$$\frac{9}{8 kh \tan\alpha} \text{ radians} .$$

When the cone is not smoothly terminated, so that $\delta \neq 0$, the evaluation of the integral in equation (67) is a more tedious task, but by again applying the asymptotic theory of Erdélyi, and retaining the first two terms in the series corresponding to P, we have

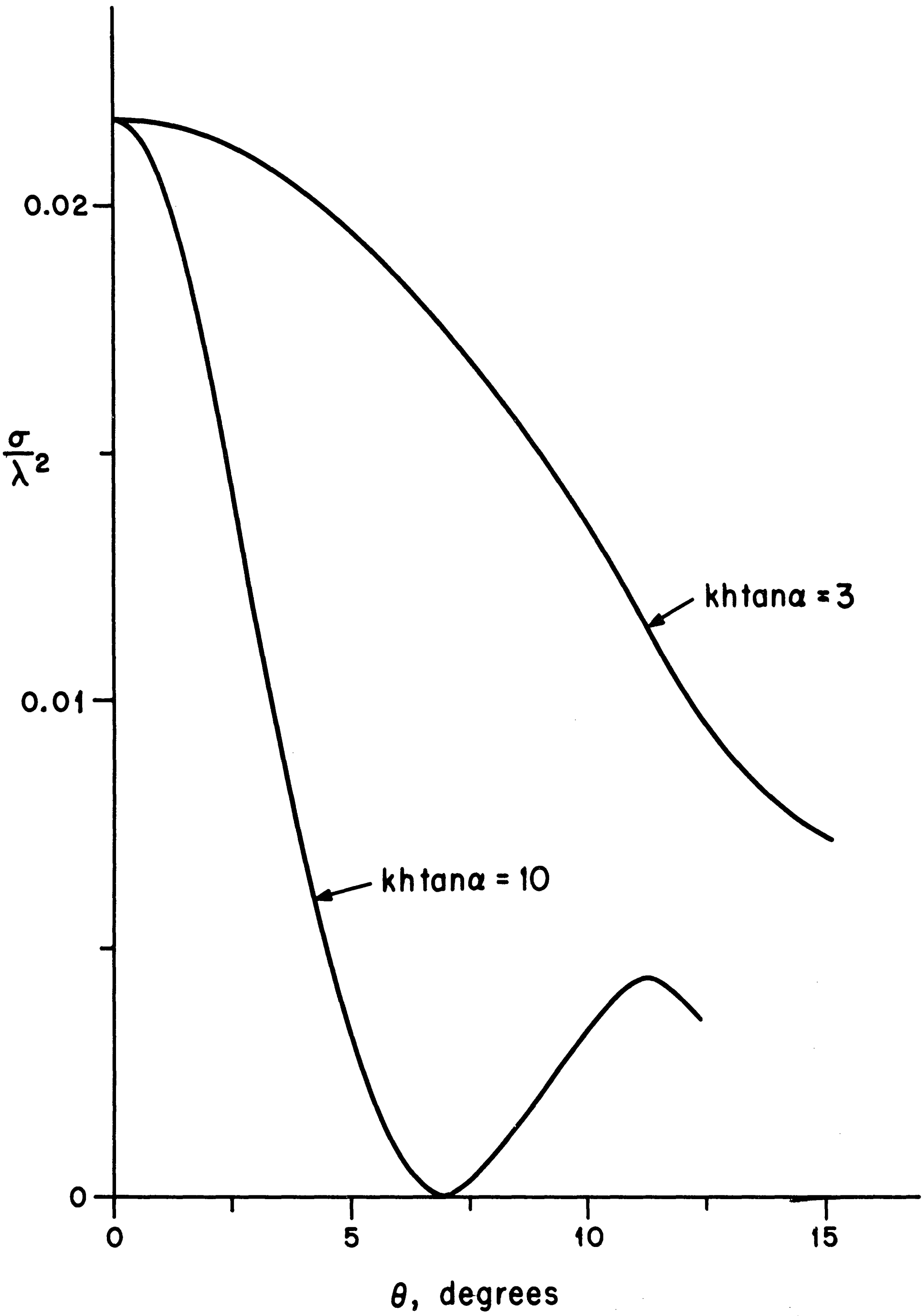

FIG. 9: BACK SCATTERING CROSS SECTION OF A CONE-SPHERE JOIN FOR $\alpha = 12\,1/2^{\circ}$: kh tan α IS THE RADIUS OF THE JOIN.

$$
\begin{aligned}
S_{join} \sim \frac{i}{8}\, e^{2ikh\cos\theta} \Bigg[\Bigg\{ & \frac{\sin\delta}{\cos(\alpha+\delta-\theta)\cos(\alpha-\theta)} \Bigg(2ikh\tan\alpha - \sin\theta \\
& - \frac{\sin\theta\cos^2\cos\delta + \frac{1}{2}\cos\theta(\cos^2\theta - \sin^2\theta)\sin(2\alpha+\delta)}{\cos(\alpha+\delta-\theta)\cos(\alpha-\theta)} \Bigg) \\
& + \frac{\cos(\alpha+\delta)}{\cos^3(\alpha+\delta-\theta)} \Bigg\} H_o^{(1)}(2kh\tan\alpha\sin\theta) \\
& + \Bigg\{ \frac{\sin\delta}{\cos(\alpha+\delta+\theta)\cos(\alpha+\theta)} \Bigg(2ikh\tan\alpha + \sin\theta \\
& + \frac{\sin\theta\cos^2\theta\cos\delta - \frac{1}{2}\cos\theta(\cos^2\theta - \sin^2\theta)\sin(2\alpha+\delta)}{\cos(\alpha+\delta+\theta)\cos(\alpha+\theta)} \Bigg) \\
& + \frac{\cos(\alpha+\delta)}{\cos^3(\alpha+\delta+\theta)} \Bigg\} H_o^{(2)}(2kh\tan\alpha\sin\theta) \Bigg] \quad . \qquad (73)
\end{aligned}
$$

This is clearly in agreement with (71) when $\delta = 0$. It is also finite for $\theta = 0$, notwithstanding the formal restriction to angles $\theta \neq 0$ inherent in the derivation, and the nose-on value can be shown to be identical to that in equation (16). Indeed, for sufficiently small δ, α and θ an adequate approximation to (73) is

$$S_{join} \sim \frac{i}{4} \sec^2\alpha\, e^{2ikh\cos\theta} (2ikh\tan\alpha\tan\delta + 1)\, J_o(2kh\tan\alpha\sin\theta) \qquad (74)$$

and the Bessel function which characterized the near nose-on behavior for a smoothly-terminated cap is still appropriate when there is a small angular discontinuity at the join, but for larger values of δ ($kh\tan\alpha|\tan\delta| \gtrsim 1$) it is necessary to go back to the full expression (73). Because of the reduced accuracy of the physical optics approximation to the surface field in the presence of a significant wedge-type singularity, the solution obtained is then of questionable worth, and in view of the complicated nature of the formulas, we shall concentrate on smoothly-terminated cones throughout the remainder of this section.

For a cone-sphere illuminated by a plane wave whose direction of incidence is within the backward cone ($\theta \leq \alpha$), a part of the cap is necessarily lit, and cannot produce a specular return unless the cone itself has generated one at a smaller angle (and even then only if $\alpha \geq \pi/4$). An expression for the join contribution was given in equation (71), and this reduces to the form shown in (72) if $kh \tan\alpha \sin\theta \ll 1$. The latter appears accurate in spite of the assumption $kh \tan\alpha \sin\theta >> 1$ employed in its derivation, but if we now apply the large argument condition uniformly, the Hankel functions in (71) can be replaced by the leading terms of their asymptotic expansions to give

$$S_{join} = \frac{i}{8\pi} \sec^2\alpha \sqrt{\frac{\lambda}{2h \tan\alpha \sin\theta}} \left\{ \frac{\cos^3\alpha}{\cos^3(\alpha+\theta)} e^{2ikh \sec\alpha \cos(\alpha+\theta) + i\pi/4} \right.$$

$$\left. + \frac{\cos^3\alpha}{\cos^3(\alpha-\theta)} e^{2ikh \sec\alpha \cos(\alpha-\theta) - i\pi/4} \right\} . \tag{75}$$

This can be interpreted physically as a sum of contributions from the extreme points of the join (see Fig. 5) and, as such, is analogous to the formula for the rim return (equation 55) in the case of a flat-backed cone. Apart from the variation represented by the quantities $\cos^3(\alpha \pm \theta)$, the contributions differ only in phase, and if it is assumed that θ is small enough* for us to neglect this variation, the amplitude of each of the contributions in (75) is smaller than that of the corresponding one in (55) by the factor

$$-2ikh \sin\alpha \cos\alpha \tan(\alpha+\theta) \simeq -2ikh \sin^2\alpha \quad ,$$

which is just the ratio of the rim return (12) to the join return (17) at nose-on incidence.

---

*This is compatible with the asymptotic expansion of the Hankel functions in (71) if $kh \tan\alpha$ is large enough.

The examples of the flat-backed cone and cone-sphere illustrate the functional transition of a ring return from the caustic or phase-coherent behavior at nose-on incidence to the sum of two similar discrete contributions at aspects away from nose-on, and it comes as no surprise that this is true for any type of ring singularity, no matter whether it occurs in the first or tenth derivative of the profile. To an accuracy which is adequate for most purposes, the physical optics approximation shows that as the aspect angle moves away from nose-on, the variation of the back scattered field is first described by the function

$$J_o(2ka \sin\theta) \quad ,$$

where a is the radius of the singularity, and for larger values of θ we can introduce the asymptotic expansion of J_o to yield a sum of contributions from those points of the singularity in the plane containing its axis of symmetry and the direction of propagation. For incidence outside the backward cone, one of these points is shadowed and its contribution must be omitted, but if the incidence is still well away from the direction $\theta = \pi/2 - \alpha$ of specular reflection from the sides of the cone, this prescription continues to provide a reasonable basis for estimating the scattering attributable to the singularity.

In the case of a flat-backed cone, the single rim return remaining outside the backward cone is identical to the scattering in the far side lobes of the specular flash, leading to a continuity in the theoretical description that is both mentally gratifying and computationally convenient. It is probable, however, that the continuity is somewhat fortuitous, and certainly it is difficult to produce the same degree of continuity in our simplified formulae for the scattering from a cone-sphere.

To see this, consider a cone-sphere illuminated by a plane wave incident in a direction θ outside the backward cone and such that $\alpha < \theta \leq \frac{\pi}{2} - \alpha$. Since physical optics is based on independent scattering from the individual surface elements, we can again treat the cone and cap separately. The scattering from the cone in this aspect range was described in equations (56) through (62), and for the spherical cap alone we refer to equation (63) which, when particularized to the case of a smooth join ($\delta = 0$), has the form

$$S^{cap} = -\frac{2i\pi}{\lambda^2}(h \sec\alpha \tan\alpha)^2 e^{2ikh\sec^2\alpha\cos\theta} \int d\phi'' \int_{\frac{\pi}{2}-\alpha}^{\gamma} (\sin\theta\sin\theta'\cos\phi''$$

$$+ \cos\theta\cos\theta')\exp\left\{-2ikh\sec\alpha\tan\alpha(\sin\theta\sin\theta'\cos\phi'' + \cos\theta\cos\theta')\right\} \times$$

$$\times \sin\theta' \, d\theta' \quad , \tag{76}$$

where $\phi'' = \phi' - \pi$ and runs over the portion of the range $(-\pi, \pi)$ corresponding to the illuminated region of the cap.

Taking first the ϕ'' integration and noting that the saddle point is $\phi'' = 0$, we can effect a steepest descents evaluation under the assumption $kh\sec\alpha\tan\alpha\sin\theta\sin\theta' >> 1$, giving

$$S^{cap} \sim -e^{-i\frac{\pi}{4}} kh\sec\alpha\tan\alpha \sqrt{\frac{h\sec\alpha\tan\alpha}{2\lambda\sin\theta}}\, e^{2ikh\sec^2\alpha\cos\theta} \times$$

$$\times \int_{\frac{\pi}{2}-\alpha}^{\frac{\pi}{2}+\theta} \sqrt{\sin\theta'}\cos(\theta'-\theta)\exp\left\{-2ikh\sec\alpha\tan\alpha\cos(\theta'-\theta)\right\} d\theta' \tag{77}$$

where this is, of course, only a first order evaluation. For the θ' integration the saddle point is $\theta' = \theta$, which is outside the range of integration except when the direction of incidence is normal to the side of the cone (i.e. $\theta = \pi/2 - \alpha$). If the incidence is well away from this direction, however, we can write

$$\sqrt{\sin\theta'}\cos(\theta'-\theta) = \left\{\sqrt{\sin\theta'}\cot(\theta'-\theta)\right\}\sin(\theta'-\theta)$$

and remove the bracketted pair of factors from the integrand at the value of θ' nearest to the saddle point, i.e. at $\theta' = \pi/2 - \alpha$. The remaining integral is then capable of exact evaluation, and hence

$$S^{cap} \sim -\frac{1}{2} e^{i\frac{\pi}{4}} \sqrt{\frac{h \tan\alpha}{2\lambda \sin\theta}} \tan(\alpha+\theta) \left\{ e^{2ikh \sec\alpha \cos(\alpha+\theta)} - e^{2ikh \sec^2\alpha \cos\theta} \right\} . \tag{78}$$

The second term is clearly a shadow boundary contribution and, being in error, is ignored as usual. Only the first term now remains, and though this is attributable to the join and is therefore presumed accurate, it is cancelled by the equal and opposite contribution (57) provided by the rim of the cone. Such cancellation is, however, only to the first order. Were we to pursue the evaluations of the cone and cap integrals to the next (lower) order in kh or, equivalently, treat the two surface integrals together and seek the leading order contribution of the sum (as was done in the derivation of the join contribution for incidence within the backward cone), we could expect to arrive at an expression for the scattering amplitude which, in the far side lobes of the specular flash, was tantamount to taking just the first term in (75). Unfortunately, no satisfactory way of obtaining this directly has been found, and to estimate the scattering in the aspect range $\alpha < \theta << \pi/2 - \alpha$ we are forced to rely on reasoning by analogy with the flat-backed cone solution.

To illustrate the nature of the cap contribution when θ is not well away from the specular direction, let us consider the results for $\theta = \pi/2 - \alpha$. Putting $\theta'' = \theta' - \theta$ and $\theta = \pi/2 - \alpha$ in equation (77), we have

$$S^{cap} \sim -e^{-i\frac{\pi}{4}} kh \sec^2\alpha \tan\alpha \sqrt{\frac{h \tan\alpha}{2\lambda}}\, e^{2ikh \sec\alpha \tan\alpha} \int_0^{\pi/2} \sqrt{\cos(\theta'' - \alpha)} \times$$
$$\times \cos\theta'' \exp\left\{-2ikh \sec\alpha \tan\alpha \cos\theta''\right\} d\theta''$$

and if $kh \sec\alpha \tan\alpha >> 1$, the two cosine factors can be removed from the integrand at the saddle point $\theta'' = 0$ and the integral evaluated by steepest descents to give

$$S^{cap} \sim -\frac{1}{4}\,kh\sec\alpha\tan\alpha \quad . \tag{79}$$

This is half the far field amplitude appropriate to a specular return from a sphere of radius $h\sec\alpha\tan\alpha$, and is the expected answer for the cap at this aspect since half of the 'required' Fresnel zone is cut off. It is, moreover, of a lower order in kh than the specular contribution (58) from the sides of the cone, so that for a cone-sphere the scattering in the direction $\theta = \pi/2 - \alpha$ is, to the first order, unaffected by the presence of the spherical cap.

Thus, for a cone-sphere of base radius b viewed at the angle $\theta = \pi/2 - \alpha$, the far field amplitude is obtainable from (58) by putting $h = b\cos\alpha\cot\alpha$, and is

$$S = \frac{kb}{3}\,e^{-i\frac{\pi}{4}}\sqrt{\frac{kb}{\pi}}\,\cot\alpha \quad . \tag{80}$$

From this we have

$$\frac{\sigma}{\lambda^2} = K'(kb)^3 \tag{81}$$

with

$$K' = \left(\frac{\cot\alpha}{3\pi}\right)^2 \tag{82}$$

(cf equations 59 and 60), and to judge from the relatively small amount of experimental data available, the above formula is quite accurate. As examples, for $\alpha = 12\,1/2^{o}$ the measured values of σ/λ^2 in the specular direction are 20.4 db (vertical polarization) and 20.9 db (horizontal polarization) when kb = 8.126, rising to 22.0 and 21.8 db respectively when kb = 8.879 (Senior, 1963). The corresponding values deduced from equation (81) are 21.0 and 22.1 db for ka = 8.126 and 8.879 respectively, and such agreement is even better than was found with the flat-backed cone. More data is, however, required before concluding that this is typical.

For aspects $\theta = \pi/2 - \alpha$ and beyond, the scattering from the flat-backed cone is, of course, reinforced by the cap return (79), and though this is insignificant at high frequencies when $\theta = \pi/2 - \alpha$, it becomes more important as θ increases owing to the fall-off in the return from the cone. At the same time, the specular return from the cap increases from the value $-\frac{1}{4}kb$ shown in (79) up to the value $-\frac{1}{2}kb$ appropriate to a complete Fresnel zone on a sphere of radius b, and to determine the rate at which this rise occurs, we go back to equation (77). Replacing θ' by $\theta'' + \theta$ and removing the trigonometric functions from the integrand at the resulting saddle point $\theta'' = 0$, we have

$$S^{cap} \sim -e^{-i\frac{\pi}{4}} kb\sqrt{\frac{b}{2\lambda}}\, e^{2ikb\,\mathrm{cosec}\,\alpha\cos\theta} \int_{\frac{\pi}{2}-\alpha-\theta}^{\frac{\pi}{2}} e^{-2ikb\cos\theta''}\, d\theta''$$

where, for convenience, we have written

$$b = h \sec\alpha \tan\alpha \quad ,$$

and a steepest descents evaluation now provides

$$S^{cap} \sim -\frac{1}{4} kb\, e^{-2ikb(1-\mathrm{cosec}\,\alpha\cos\theta)} \left\{1 + \frac{2x}{\sqrt{\pi}} e^{i(x^2-\pi/4)} \mathfrak{T}(x)\right\} \tag{83}$$

where

$$x = \sqrt{kb}\,(\theta + \alpha - \frac{\pi}{2}) \tag{84}$$

and $\mathfrak{T}(x)$ is the previously-defined function related to the Fresnel integral. Since $\mathfrak{T}(0) = 1$, S^{cap} reduces to the form shown in equation (79) when $x = 0$ (i.e., $\theta = \pi/2 - \alpha$), and for small $x > 0$

$$S^{cap} \sim -\frac{1}{4} kb\, e^{-2ikb(1-\mathrm{cosec}\,\alpha\cos\theta)} \left\{1 + \frac{2x}{\sqrt{\pi}} e^{i(x^2-\pi/4)} + O(x^2)\right\} . \tag{85}$$

On the other hand, for large x

$$\mathcal{F}(x) \sim \frac{\sqrt{\pi}}{2x} e^{i(\pi/4 - x^2)} + \frac{1}{2ix^2} ,$$

in which case

$$S^{cap} \sim -\frac{1}{2} kb\, e^{-2ikb(1 - \mathrm{cosec}\,\alpha \cos\theta)} \left\{1 - \frac{i}{2x\sqrt{\pi}} e^{i(x^2 - \pi/4)} + O(x^{-2})\right\} \quad (86)$$

and S^{cap} is within (about) 10 percent of the full specular value represented by the first term on the right of (86) if

$$\theta - (\frac{\pi}{2} - \alpha) \gtrsim \sqrt{\frac{\lambda}{b}} .$$

For a cone-sphere viewed at an aspect $\theta \geq \pi/2 - \alpha$, the effect of the cap contribution is to reinforce the scattering from the sides of the cone. Though its magnitude is less than S^{cone} if $\theta = \pi/2 - \alpha$, it becomes ever more important as θ increases, serving to raise the overall scattering in the further side lobes of the cone's flash, and ultimately to level out the net return at the value appropriate to a specular contribution from a sphere of radius b. However, the cap also has an effect if $\theta < \pi/2 - \alpha$, and to determine this we again go back to equation (77). Since $\pi/2 - \alpha - \theta > 0$, the trigonometric factors are removed from the integrand at the value of θ' nearest to the saddle point, i.e. at $\theta' = \pi/2 - \alpha$, but this apart the analysis parallels that presented above for $\theta \geq \pi/2 - \alpha$, and gives

$$S^{cap} \sim -\frac{1}{4} kb \sqrt{\frac{\cos\alpha}{\sin\theta}} \sin(\alpha + \theta)\, e^{-2ikb(1 - \mathrm{cosec}\,\alpha \cos\theta)}$$

$$\cdot \left\{1 + \frac{2x}{\sqrt{\pi}} e^{i(x^2 - \pi/4)} \mathcal{F}(-x)\right\} \quad (87)$$

where x is defined in equation (84) and is now negative.

This expression for the cap contribution becomes identical to those given in equations (79) and (83) when x = 0 (i.e., $\theta = \pi/2 - \alpha$), but for small $x < 0$,

$$S^{cap} \sim -\frac{1}{4} kb \sqrt{\frac{\cos\alpha}{\sin\theta}} \sin(\alpha+\theta)\, e^{-2ikb(1-\operatorname{cosec}\alpha\cos\theta)} \times$$

$$\times \left\{ 1 + \frac{2x}{\sqrt{\pi}} e^{i(x^2-\pi/4)} + O(x^2) \right\} \tag{88}$$

(cf equation 85) . For larger $|x|$, however,

$$S^{cap} \sim -\frac{1}{2} e^{-i\frac{\pi}{4}} \sqrt{\frac{b\cos\alpha}{2\lambda\sin\theta}} \frac{\sin(\alpha+\theta)}{\frac{\pi}{2}-\alpha-\theta} e^{-2ikb(1-\operatorname{cosec}\alpha\cos\theta)+ikb(\pi/2-\alpha-\theta)^2} \tag{89}$$

which represents the contribution of the cap at aspects forward of the direction of specular scattering from the cone. As such, (89) should be identical to the first term on the right hand side of (78), and if $\frac{\pi}{2} - \alpha - \theta$ is not too large, so that we can write

$$\frac{\pi}{2} - \alpha - \theta \simeq \cos(\alpha+\theta),$$

the equivalence can be established. But this contribution is just the negative of that provided by the cone itself, and thus, to the order in kh given here, the overall return from the cone-sphere is zero. We are therefore back to the discontinuity referred to earlier, and though we have already shown that for $\alpha < \theta << \frac{\pi}{2} - \alpha$ the join contribution is represented by the leading term on the right hand side of (75), a first order analysis applied to the integral expressions for S^{cone} and S^{cap} separately is not sufficient to obtain this explicitly, nor is there any straight forward method whereby we can treat $S^{cone} + S^{cap}$ at aspects near to the flash direction in such a way as to achieve the desired continuity in our simplified formulae for the scattering.

REFERENCES

Crispin, J.W., Jr., R.F. Goodrich and K.M. Siegel 1959 "A Theoretical Method for the Calculation of the Radar Cross Sections of Aircraft and Missiles," The University of Michigan Radiation Laboratory Report No. 2591-1-H (July 1959).

Dawson, T.W.G., J.G.W. Miller and W.R. Turner 1960 "Radar Echoes from Bodies of Circular Cross Section Using Wedge Theory," Royal Aircraft Establishment, Farnborough, England Technical Note No. RAD 787 (September 1960).

Erdélyi, A. 1956 Asymptotic Expansions (Dover Publications, Inc., New York).

Felsen, L.B. 1955 "Backscattering from Wide-Angle and Narrow-Angle Cones," J.Appl. Phys. 26, pp 138-151.

Felsen, L.B. 1957 "Plane Wave Scattering by Small-Angle Cones," IRE Trans. AP-5, pp 121-129.

Gent, H., J.S. Hey and P.G. Smith 1960 "The Echoing Area of 15° Semi-Angle Cone-Spheres with Sphere Radii Between One and Two Wavelengths," presented at the Symposium on the Echoing Properties of Missiles, Farnborough, England. SECRET.

Jahnke, E. and F. Emde 1945 Tables of Functions with Formulas and Curves (Dover Publications, Inc., New York).

Keys, J.E. and R.I. Primich 1959a "The Radar Cross Section of Right Circular Metal Cones: I," Defense Research Telecommunications Establishment Report No. 1010 (May 1959).

Keys, J.E. and R.I. Primich 1959b "The Radar Cross Section of Right Circular Metal Cones: II," Defense Research Telecommunications Establishment Report No. 1023 (August 1959).

Kleinman, R.E. and T.B.A. Senior 1963 "Diffraction and Scattering by Regular Bodies - II: the Cone," The University of Michigan Radiation Laboratory Report No. 3648-2-T (January 1963).

Ruehr, O.G. 1963 "Asymptotic Evaluation of Physical Optics Integrals for Cone-Sphere," The University of Michigan Radiation Laboratory Memorandum No. 2500-286 (January 1963).

Senior, T.B.A. 1963 "Cross Sections of Nose Cones," The University of Michigan Radiation Laboratory Report No. 5212-1-F (January 1963). CONFIDENTIAL.

REFERENCES
(continued)

Senior, T.B.A. 1965 "Analytical and Numerical Studies of the Back Scattering Behavior of Spheres," The University of Michigan Radiation Laboratory Report No. 7030-1-T (June 1965).

Siegel, K.M. 1963 "Radar Cross Section of a Cone-Sphere," Proc. IEEE (Correspondence) 51, pp 231-232.

Spencer, R C 1951 "Back Scattering from Conducting Surfaces," Air Force Cambridge Research Center Report No. E5070.

DISTRIBUTION LIST, F 04694-67-C-0055, TECHNICAL REPORTS

Aerospace Corporation ATTN: H. J. Katzman, Bldg. 537, Room 1007 P. O. Box 1308 San Bernardino, CA 92402	Copies 1 - 10 (incl.)
Air Force Cambridge Research Laboratories ATTN: R. Mack CRDG L. G. Hanscom Field Bedford, MA 01730	Copies 11, 12.
Advanced Research Projects Agency ATTN: W. Van Zeeland The Pentagon Washington, DC 20301	Copies 13, 14.
Air University Library ATTN: AU Maxwell AFB, AL 36112	Copy 15
Air Force Avionics Laboratory ATTN: William F. Bahret - AVWE-2 Wright-Patterson AFB, OH 45433	Copy 16
Space and Missile Systems Organization ATTN: Capt. J. Wheatley, BSYDP Norton AFB, CA 92409	Copies 17, 18.
Space and Missile Systems Organization ATTN: BSYLD Norton AFB, CA 92409	Copies 19, 20.
Electronic Systems Division (AFSC) ATTN. Lt. Nyman ESSXS L. G. Hanscom Field Bedford, MA 01730	Copy 21

DISTRIBUTION LIST, F 04694-67-C-0055, TECHNICAL REPORTS (continued)

Institute for Defense Analyses ATTN: Classified Library 400 Army-Navy Drive Alexandria, VA 22202	Copy 22
MIT-Lincoln Laboratory Representative P. O. Box 4188 Norton AFB, CA 92409	Copy 23
MIT-Lincoln Laboratory BMRS Project Office P. O. Box 73 Lexington, MA 02173	Copy 24
MIT-Lincoln Laboratory ATTN: S. Borison P. O. Box 73 Lexington, MA 02173	Copy 25
MIT-Lincoln Laboratory ATTN: J. Rheinstein P. O. Box 73 Lexington, MA 02173	Copy 26
MITRE Corporation ATTN: P. Waterman Bedford, MA 01730	Copy 27
North American Space and Information Systems ATTN: S. Wozniak Tulsa, OK 73100	Copy 28
Special Projects Office, Bureau of Weapons ATTN: M. Blum Washington, DC 20301	Copies 29, 30, 31
Northrop-Norair Division ATTN: F. K. Oshiro 3901 W. Broadway Hawthorne, CA 90250	Copy 32
DRC, Inc. P. O. Box 3587 Santa Barbara, CA 93105	Copy 33
Defense Documentation Center, Cameron Station Alexandria, VA 22314	Copies 34 - 53 (incl).

....

UNCLASSIFIED

Security Classification

DOCUMENT CONTROL DATA - R&D

(Security classification of title, body of abstract and indexing annotation must be entered when the overall report is classified)

1. ORIGINATING ACTIVITY (Corporate author)	2a. REPORT SECURITY CLASSIFICATION
The University of Michigan Radiation Laboratory Department of Electrical Engineering Ann Arbor, Michigan 48108	UNCLASSIFIED
	2b. GROUP

3. REPORT TITLE

PHYSICAL OPTICS APPLIED TO CONE-SPHERE-LIKE OBJECTS

4. DESCRIPTIVE NOTES (Type of report and inclusive dates)

Technical Report No. 2

5. AUTHOR(S) (Last name, first name, initial)

SENIOR, Thomas B. A.

6. REPORT DATE	7a. TOTAL NO. OF PAGES	7b. NO. OF REFS
May 1967	57	15

8a. CONTRACT OR GRANT NO.	9a. ORIGINATOR'S REPORT NUMBER(S)
F 04694-67-C-0055	8525-2-T
b. PROJECT NO.	
c.	9b. OTHER REPORT NO(S) (Any other numbers that may be assigned this report)
d.	BSD TR 67 182

10. AVAILABILITY/LIMITATION NOTICES This document is subject to special export controls. Transmittal to foreign governments or nationals may be made only with prior approval of SAMSO (SMSDI), Los Angeles AF Station, Los Angeles Calif 90045.

11. SUPPLEMENTARY NOTES	12. SPONSORING MILITARY ACTIVITY
	Space and Missile Systems Organization (AFSC) Norton AFB, California, 92409

13. ABSTRACT

The physical optics method is applied to a variety of cone-sphere-like objects, and the resulting expressions for the back scattered field are examined.

DD FORM 1 JAN 64 1473

UNCLASSIFIED

Security Classification

14. KEY WORDS	LINK A		LINK B		LINK C	
	ROLE	WT	ROLE	WT	ROLE	WT
RADAR CROSS SECTIONS BACK SCATTER POINTED OBJECTS THEORY PHYSICAL OPTICS						

INSTRUCTIONS

1. ORIGINATING ACTIVITY: Enter the name and address of the contractor, subcontractor, grantee, Department of Defense activity or other organization *(corporate author)* issuing the report.

2*a*. REPORT SECURITY CLASSIFICATION: Enter the overall security classification of the report. Indicate whether "Restricted Data" is included. Marking is to be in accordance with appropriate security regulations.

2*b*. GROUP: Automatic downgrading is specified in DoD Directive 5200.10 and Armed Forces Industrial Manual. Enter the group number. Also, when applicable, show that optional markings have been used for Group 3 and Group 4 as authorized.

3. REPORT TITLE: Enter the complete report title in all capital letters. Titles in all cases should be unclassified. If a meaningful title cannot be selected without classification, show title classification in all capitals in parenthesis immediately following the title.

4. DESCRIPTIVE NOTES: If appropriate, enter the type of report, e.g., interim, progress, summary, annual, or final. Give the inclusive dates when a specific reporting period is covered.

5. AUTHOR(S): Enter the name(s) of author(s) as shown on or in the report. Enter last name, first name, middle initial. If military, show rank and branch of service. The name of the principal author is an absolute minimum requirement.

6. REPORT DATE: Enter the date of the report as day, month, year; or month, year. If more than one date appears on the report, use date of publication.

7*a*. TOTAL NUMBER OF PAGES: The total page count should follow normal pagination procedures, i.e., enter the number of pages containing information.

7*b*. NUMBER OF REFERENCES: Enter the total number of references cited in the report.

8*a*. CONTRACT OR GRANT NUMBER: If appropriate, enter the applicable number of the contract or grant under which the report was written.

8*b*, 8*c*, & 8*d*. PROJECT NUMBER: Enter the appropriate military department identification, such as project number, subproject number, system numbers, task number, etc.

9*a*. ORIGINATOR'S REPORT NUMBER(S): Enter the official report number by which the document will be identified and controlled by the originating activity. This number must be unique to this report.

9*b*. OTHER REPORT NUMBER(S): If the report has been assigned any other report numbers *(either by the originator or by the sponsor)*, also enter this number(s).

10. AVAILABILITY/LIMITATION NOTICES: Enter any limitations on further dissemination of the report, other than those imposed by security classification, using standard statements such as:

(1) "Qualified requesters may obtain copies of this report from DDC."

(2) "Foreign announcement and dissemination of this report by DDC is not authorized."

(3) "U. S. Government agencies may obtain copies of this report directly from DDC. Other qualified DDC users shall request through
____ ."

(4) "U. S. military agencies may obtain copies of this report directly from DDC. Other qualified users shall request through
____ ."

(5) "All distribution of this report is controlled. Qualified DDC users shall request through
____ ."

If the report has been furnished to the Office of Technical Services, Department of Commerce, for sale to the public, indicate this fact and enter the price, if known.

11. SUPPLEMENTARY NOTES: Use for additional explanatory notes.

12. SPONSORING MILITARY ACTIVITY: Enter the name of the departmental project office or laboratory sponsoring *(paying for)* the research and development. Include address.

13. ABSTRACT: Enter an abstract giving a brief and factual summary of the document indicative of the report, even though it may also appear elsewhere in the body of the technical report. If additional space is required, a continuation sheet shall be attached.

It is highly desirable that the abstract of classified reports be unclassified. Each paragraph of the abstract shall end with an indication of the military security classification of the information in the paragraph, represented as *(TS)*, *(S)*, *(C)*, *or (U)*.

There is no limitation on the length of the abstract. However, the suggested length is from 150 to 225 words.

14. KEY WORDS: Key words are technically meaningful terms or short phrases that characterize a report and may be used as index entries for cataloging the report. Key words must be selected so that no security classification is required. Identifiers, such as equipment model designation, trade name, military project code name, geographic location, may be used as key words but will be followed by an indication of technical context. The assignment of links, rules, and weights is optional.